Impacts of maritime shipping on air pollution along the U.S. East Coast

Maryam Golbazi[1] and Cristina Archer[1]

[1]Center for Research in Wind (CReW), University of Delaware, 221 Academy Street, Newark, DE 19716, USA

Correspondence: Maryam Golbazi, Center for Research in Wind (CReW), University of Delaware, 221 Academy Street, Newark, DE 19716, USA (mgolbazi@udel.edu)

Abstract.

Air pollution is considered a leading threat to human health in the U.S. and worldwide. An important source of air pollution in coastal areas is the globally increasing maritime shipping traffic. In this study, we take a high-resolution modeling approach to investigate the impacts of ship emissions on concentrations of various atmospheric pollutants, under the meteorological conditions and emissions of the year 2018. We utilize the Comprehensive Air Quality Model with extensions (CAMx) to simulate transport, diffusion, and chemical reactions, and the Weather Research and Forecasting (WRF) model to provide the meteorological inputs. We focus on four criteria pollutants – fine particulate matter with a diameter smaller than $2.5\,\mu m$ ($PM_{2.5}$), nitrogen dioxide (NO_2), sulfur dioxide (SO_2), and ozone (O_3) – as well as nitrogen oxide (NO), and we calculate their concentrations in the presence and absence of the ship emissions along the U.S. East Coast, particularly in the proximity of major ports.

We find that ship emissions increase the $PM_{2.5}$ concentrations over the ocean and sparse areas inland. The 98-th percentile of the 24-hour average $PM_{2.5}$ concentrations (the "design value" used by the U.S. Environmental Protection Agency) increased by up to $3.2\,\mu g\,m^{-3}$ in some coastal areas. In addition, ships contribute significantly to SO_2 concentrations, up to 95% over the Atlantic and up to 90% over land in coastal states, which represents a ~45 ppb increase in the SO_2 design values in some states. The 98-th percentile of the hourly NO_2 concentrations also increased by up to 15 ppb at the major ports and along the shore. In addition, we find that the impact of shipping emissions on O_3 concentrations is not uniform, meaning that ships affect ozone pollution in both positive and negative ways. Over the ocean, O_3 concentrations were significantly higher in the presence of ships, but in major coastal cities O_3 concentrations decreased in the presence of ships. Our simulation results show that ships emit significant amounts of fresh NO in the atmosphere, which then helps scavenge O_3 in VOC-limited areas, such as major ports. By contrast, over the ocean (NO_x-limited regime), enhanced NO_x concentrations due to ships contribute to the formation of O_3 and therefore enhance O_3 concentrations. Overall, due to the dominant southwesterly wind direction in the region, the impacts of ships on air pollutants mainly remain offshore. However, in coastal states near major ports, the impacts are significantly important.

1 Introduction

Globally, it is estimated that, in 2019, ambient air pollution, particularly particulate matter (PM) and ozone (O_3), was responsible for 4.5 million premature deaths worldwide (Fuller et al., 2022). This ranked air pollution as a leading risk factor in the Global Burden of Disease Study by the Institute for Health Metrics and Evaluation in 2019 (Murray and Lopez, 1996). Meanwhile, ship traffic is globally increasing and is becoming an important source of air pollution, especially in coastal areas (Corbett and Fischbeck, 1997; Eyring et al., 2010b; Schnurr and Walker, 2019). Sea transport accounts for 80% of goods transported worldwide (Schnurr and Walker, 2019), while recent studies estimate demand growth of almost 40% for seaborne trade by 2050 (Serra and Fancello, 2020). Marine vessels are important sources of air pollutants, emitting sulfur oxides (SO_x), nitrogen oxides ($NO_x = NO + NO_2$), particulate matter (PM), carbon monoxide (CO), volatile organic compounds (VOC), and carbon dioxide (CO_2) (Corbett et al., 2007; Eyring et al., 2007a; Eyring, 2008; Smith et al., 2015). Low-grade marine fuel oil contains 3,500 times more sulfur than road diesel (Wan et al., 2016). Studies report fuel consumption of ocean-going ships between 200-290 million metric tons for the year 2000 (Corbett and Köhler, 2003; Endresen et al., 2007). Ships are responsible for about 15% of all global anthropogenic NO_x emissions and 4–9% of sulfur dioxide SO_2 emissions. In addition, oceangoing ships are estimated to emit 1.2–1.6 million metric tons (Tg) of PM annually (Corbett et al., 2007; Eyring et al., 2010b; Viana et al., 2014).

About 70% of ship emissions occur within 400 km of the shore (Corbett et al., 1999; Eyring et al., 2005; Endresen et al., 2003). Thus, ships can be a major source of pollution in coastal areas and can impact human health. For instance, ship emissions in East Asia have caused 14,500–37,500 premature deaths in 2013, the amount of which had doubled since 2005 (Liu et al., 2016). Similarly, particulates emitted from ships cause 60,000 cardiopulmonary and lung cancer deaths each year worldwide (Corbett et al., 2007). Studies from different parts of the world like China show that shipping emissions increased the annual averaged $PM_{2.5}$ concentrations in the eastern coastal regions up to $5.2\,\mu g\,m^{-3}$, which was carried 900 km inland (Lv et al., 2018). In Europe, although the increase in $PM_{2.5}$ concentrations by ships is found to be small, their relative contribution is large because of the low background $PM_{2.5}$ concentrations (Viana et al., 2009; Aksoyoglu et al., 2016).

Fine particulate matter ($PM_{2.5}$) is a harmful air pollutant that consists of microscopic particles with a diameter smaller than $2.5\,\mu m$. These particles can penetrate human lungs and even the bloodstream and cause serious health problems (U.S. Environmental Protection Agency (EPA), 2020b). NO_x are a group of highly reactive gases; although seven compounds are technically part of the NO_x family (NO, NO_2, nitrous oxide N_2O, dinitrogen dioxide N_2O_2, dinitrogen trioxide N_2O_3, dinitrogen tetroxide N_2O_4, dinitrogen pentoxide N_2O_5), the most abundant are NO and NO_2, but only NO_2 is actually regulated in the U.S. NO_2 is harmful to humans by irritating the human respiratory system and to the environment by creating acid rain (U.S. Environmental Protection Agency (EPA), 2020a; Lin and McElroy, 2011); it is also a precursor to tropospheric ozone (O_3) formation, which has further negative impacts on human health (, EPA). Similarly, short-term exposure to SO_2 can harm the human respiratory system. These four pollutants – $PM_{2.5}$, SO_2, NO_2, and O_3 – are both primary (i.e., they can be directly emitted into the atmosphere) and secondary (i.e., they can also form after chemical reactions in the atmosphere) pollutants. Here, we will focus on these four pollutants which are among the seven "criteria" pollutants that are regulated at the federal level by the

U.S. Environmental Protection Agency (EPA) via the National Ambient Air Quality Standards (NAAQS)(U.S. Environmental Protection Agency (EPA), 2022b).

Due to the complex nature of the atmosphere and its processes, such as chemical reactions, transport, and diffusion, high concentrations of these pollutants are not necessarily found where their emissions are highest. Therefore, although the ship emissions are released in marine environments, the atmospheric conditions can play an essential role in transporting those pollutants, some of which are precursors for the formation of secondary EPA-regulated pollutants, like O_3.

Ozone pollution is one of the main focuses of this study. The rate of ozone production can be limited by the concentration of either VOC or NO_x and depends on the relative sources of hydroxyl radical (OH) and NO_x (Finlayson-Pitts and Pitts Jr, 1993). When the rate of OH production is greater than the rate of NO_x production, the rate of ozone production is NO_x-limited. In this situation, ozone concentrations are sensitive to NO_x emissions rather than VOC concentrations. In contrast, when the rate of OH production is less than the rate of NO_x production, ozone production is VOC-limited. In this case, ozone is most effectively reduced by lowering VOC concentrations. NOx is generally higher where human mobility and transportation are higher (Archer et al., 2020) and While O_3 is generally NO_x-limited in rural areas and downwind suburban areas, in urban areas with high population and high traffic emissions O_3 is often VOC-limited (Seinfeld and Pandis, 1998). Motor vehicles are among the major sources of ozone pollution in the region through their NO_x and VOC emissions (Niemeier et al., 2006; Yao et al., 2015; Zhang et al., 2014). However, the impact of ocean ship emissions along the East Coast of the United States is lacking in the literature and we fill this gap in this study. In locations that exceed the EPA ozone standards by only 2-3 ppb, like the small state of Delaware (Moghani et al., 2018), the ship contribution could be of even higher importance.

Here, we explore the impacts of ocean-going ship emissions on the air quality along the U.S. East Coast by utilizing the Comprehensive Air Quality Model with extensions (CAMx) for our simulations. For the first time, we use the most recent high spatial (4 km) and temporal (hourly) resolution ship emission data from the EPA's National Emission Inventory (NEI). We also include the ship stack height to consider at what vertical layer the emissions are emitted into the atmosphere, to be able to account for stability and atmospheric impacts on the pollutants. We investigate the pollution concentrations in a control scenario based on the shipping emissions in the year 2018. Then, we conduct another simulation for a hypothetical condition where we eliminate the ship emissions altogether while keeping everything else the same. The difference between the two scenarios gives insights into the net contribution of the ships to air pollution.

Seasonal variations in the impact of shipping on various pollutants have been documented in prior studies. For example, Eyring et al. (2010) noted that during Mediterranean summer conditions, characterized by slow atmospheric transport, strong solar radiation, and limited washout, primary ship emissions accumulate, and secondary pollutants form. They reported that secondary sulfate aerosols from shipping were responsible for 54% of the average sulfate aerosol concentration in the region during the summer. Our findings along the US East Coast align with these results, highlighting the substantial contribution of ships to SO_2 pollution during the summer season. Furthermore, they observed that in winter, shipping NOx emissions could lead to ozone depletion in northern Europe (Eyring et al., 2010a). In a separate study, Eyring et al., (2007) noted significant variations in simulated O_3 levels between January and July, despite a consistent ship emission inventory throughout the year. They found that during winter, additional NOx emissions from shipping led to O_3 reduction due to titration, while in summer,

these emissions resulted in relatively modest but positive O_3 concentration changes in regions with sufficient solar radiation. They also show that the highest ship impacts on O_3 due to the ship emissions were found in July and April, whereas in October and January, the impacts were smaller (Eyring et al., 2007b). In this study, however, we base our analysis on the summer (June 1st – August 31st) when the highest O_3 episodes occur.

2 Methods

2.1 Setup of the WRF-CAMx modeling system

We take a modeling approach to explore the pollution concentration across the study domain. The models used in this study are the Weather Research and Forecasting (WRF) model, version 4.3, and the Comprehensive Air quality Model with extensions (CAMx) version 7.1 with the Carbon Bond version 6 revision 5 (CB6r5) chemical mechanism. WRF is developed at the National Center for Atmospheric Research (NCAR) (Skamarock et al., 2019) and is one of the most widely used numerical weather prediction models. CAMx is a modular, Eulerian, 3-dimensional photochemical air quality model (Ramboll Environment and Health, 2020) that simulates the emission, production, advection, diffusion, chemical transformation, and removal of atmospheric pollutants at regional scales and is among the few that are recommended by the EPA for regulatory purposes (U.S. Environmental Protection Agency (EPA), 2022a). We use the WRF-CAMx modeling system to conduct simulations of two separate scenarios, based on the exact same setup and inputs: the first scenario includes the ship emissions (WithShips) while in the second hypothetical scenario we remove the ship emissions altogether (NoShips). The difference in pollution levels between the two cases provides the net contribution of ship emissions to regional air quality.

CAMx requires input data to characterize meteorology and chemistry, initial and boundary conditions for all the modeling domains, and other environmental conditions such as the photolysis rates. Meteorology is an essential factor in the formation of many secondary pollutants, both directly and indirectly. Atmospheric stability plays a significant role in determining pollutant faith (Arya et al., 1999). In CAMx, the plume rise calculations for point sources including the CMV emissions depend on meteorological conditions and atmospheric stability to determine what vertical layer the emissions are emitted in. In the summertime, various atmospheric stabilities have been found to be dominant over the Atlantic Ocean depending on different locations (Golbazi et al., 2022; Golbazi and Archer, 2019; Archer et al., 2016). We use the WRF model to provide meteorological inputs to CAMx. The publicly available WRF-CAMx data processing program (Ramboll Environment and Health, 2020) is used to generate CAMx meteorological input files from WRF output files. Details on the WRF model setup are provided in Table 1. Our period of study is the summer of 2018, selected to reflect the most recent emission inventory available (discussed next in Section 2.2). Photolysis rate inputs to CAMx were calculated using the Tropospheric Ultraviolet and Visible (TUV) radiative transfer and photolysis model (https://www2.acom.ucar.edu/modeling/tropospheric-ultraviolet-and-visible-tuv-radiation-model).

Table 1. Details of the WRF-CAMx model setup.

Simulation period	1 June – 30 August, 2018
Horizontal grid resolution	4 km
Vertical layers	35
Lowest model level	3.5 m AMSL
Spin-up time	48 hours
WRF version 4.3	
Initial/boundary conditions	NAM reanalysis, 6-hourly, 12-km resolution
LSM	Noah-modified 21-category IGBP-MODIS
PBL Scheme	MYNN2
Shortwave radiation	RRTMG shortwave
Longtwave radiation	RRTMG scheme
SST update	NASA-JPL 1km resolution data
Grid size	400×400 grid cells
CAMx version 7.1	
Chemistry	Carbon bond 6 revision 5
Meteorological inputs	WRF model v4.3
Emission data	EPA/NEI 2018
CMV emissions	Inline point sources
Initial/boundary conditions	EPA 2018
Grid size	315×300 grid cells

    The domain of this study covers the East Coast of the United States (Figure 1) and includes major cities and highly populated regions. Furthermore, it contains several major ports, which are found to experience high shipping traffic. The meteorological files have 400×400 horizontal grid points covering the entire CAMx domain, which consists of 315×300 grid points, the same as the emission files. We impose 35 vertical levels that are closely spaced near the surface and then gradually expand. The top hydrostatic pressure is 20 hPa and the lowest model level is at approximately 3.5 m above mean sea level (AMSL). Details about the model configuration are discussed in Table 1. Both the WRF and CAMx models have a 4-km horizontal resolution, the same as the emission inventory, in order to avoid spatial interpolation of gridded emissions data. To minimize the impacts of the initial conditions on modeling results, we consider at least 48 hours of spin-up time for both models. Furthermore, as the areas of interest are far from the boundaries, the effects of boundary conditions on modeling results are expected to be minimal.
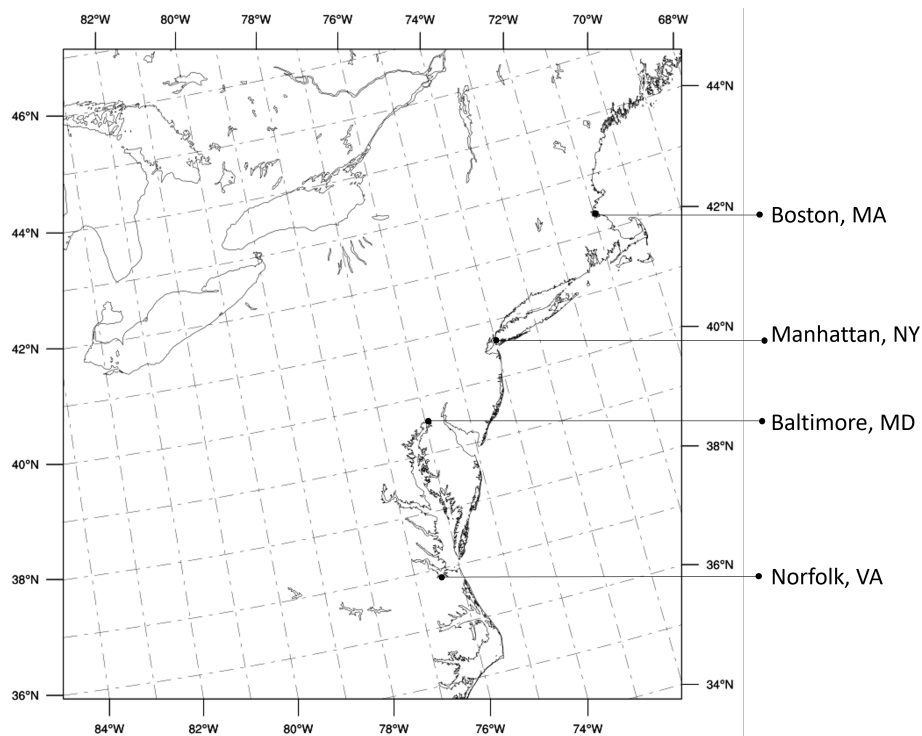
Figure 1. The study domain with 315×300 grid cells and 4-km horizontal grid resolution.

2.2 Emission data

For emission inputs, we use the most recent emission inventory (LISTOS) developed by the EPA, which includes the period May 1st, 2018 to October 1st, 2018 (U.S. Environmental Protection Agency (EPA), 2017) at 4-km horizontal grid resolution and hourly temporal resolution. The emissions are distributed on a 315×300 grid, which covers the entire East Coast of the U.S. (Figure 1), with 35 layers vertically. Emissions are treated in two basic ways within CAMx: gridded 2D emissions that are released into each grid cell of the modeling domain near the surface (i.e., "area sources", such as traffic or residential heating) and stack-specific "point sources", where each stack is assigned unique coordinates and parameters (i.e., smokestacks or ship chimneys). For inline point source emissions, CAMx computes the plume rise using stack parameters and the hourly emissions for each emission sector.

The 2018 NEI data is based on the year 2017 activity. It contains merged gridded 2D surface emissions, meaning that they are provided as one set of surface emissions that include all the existing 2D emission sectors such as all anthropogenic emissions, aircraft emissions, on-road and non-road emissions, railroad emissions, and agricultural emissions. It also includes biogenic emissions. The 2018 inventory lacks the wildfire emissions for this time and domain. However, our investigation through the wildfire history shows that 2018 was a year with a low number of wildfires especially along the East Coast (https://www.nifc.gov/fire-information/statistics/wildfires) and therefore we do not believe this to significantly impact our

findings. Nonetheless, in future studies, including wildfire emissions upon availability is recommended. In contrast to the 2D gridded emissions, the elevated point sources in this inventory are provided for each sector, separately.

For the ship emissions, we use the emission data for the Commercial Marine Vessels (CMV) sector, which includes Category 1, 2 (small engine), and 3 (large engine) ships. These emissions are calculated based on the ship's fuel consumption, ship engine type, ship activity, and emission factors specific to those characteristics. EPA's CMV estimates are computed using detailed satellite-based automatic identification system (AIS) activity data from the US Coast Guard ((U.S. Environmental Protection Agency, 2021, 2020)). Other point sources present in this inventory include electric generation units, point oil, and gas sources, and any other point sources. CAMx computes the time-varying buoyant plume rise using stack parameters and the hourly emissions for each emissions sector, including CMV. Unlike previous EPA data sets, the CMV emissions in 2018 are at a one-hour temporal resolution, which is very important and makes this study the first to utilize hourly emissions for the ships. The initial and boundary conditions for this study are also provided by the EPA and are products of the GEOS-Chem model.

The spatial distribution of the 2D gridded merged anthropogenic emissions are illustrated in Figure 2. It's important to note that O_3 is a secondary pollutant, meaning it isn't directly emitted into the atmosphere. Conversely, $PM_{2.5}$ is either a primary or secondary pollutant. Hence, we have specifically generated gridded emission maps for NO_2 and SO_2, only. The distribution of NO_2 emissions closely mirrors the pattern of major highways and roads, as transportation stands out as one of the most significant sources of nitrogen oxides (NOx) emissions. The objective of this figure is to explain the spatial distribution of gridded anthropogenic emissions, shedding light on how concentrations change (Figures 6a and 7a) in relation to their emission sources.
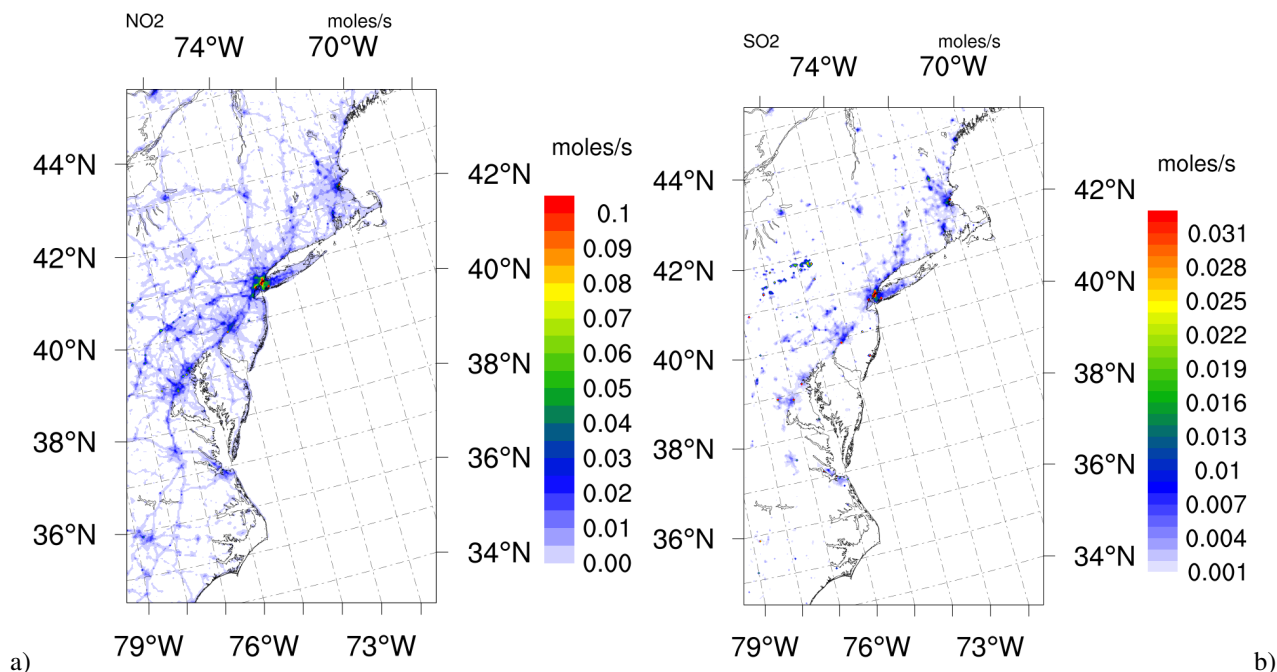
Figure 2. Gridded 2D emission distribution across the domain (averaged over time) in moles/s for a) NO$_2$, and b) SO$_2$. The gridded emissions include all the 2D anthropogenic and biogenic emissions and exclude the elevated point sources.

3   CAMx model performance analysis

The primary goal of this study is to explore changes to pollution levels between the two examined case studies, one involving the presence of ships and the other without. Despite the instances where CAMx may either under or overestimate pollutant concentrations, it is noteworthy that the model bias remains the same in both scenarios. Consequently, we hold the view that these outcomes are unlikely to have a significant influence on our analysis. Nevertheless, we have thoroughly evaluated the model's performance to maintain transparency in our findings. It's important to acknowledge that uncertainties in air quality modeling can arise from various sources, such as uncertainties in emission inventories ((Foley et al., 2015)), the accuracy of meteorological inputs (Kumar et al., 2019; Ryu et al., 2018; Zhang et al., 2007), numerical noise inherent in the model (Ancell et al., 2018; Golbazi et al., 2022), and numerical approximations.

For our evaluation process of these four pollutants, we rely on measurement data sourced from the Environmental Protection Agency (EPA) AirNow program, which is publicly accessible (https://aqs.epa.gov/aqsweb/documents/data_api.html). Within the geographical scope of our study, we have access to data from a network of monitoring stations. Specifically, there are a total of 196 stations providing data for O3, and 87, 73, and 118 stations supplying data for SO$_2$, NO$_2$, and PM$_{2.5}$, respectively. This extensive dataset forms the basis of our assessment, enabling us to comprehensively evaluate the CAMx model's performance in replicating real-world air quality conditions for these pollutants. It is worth mentioning that evaluating PM$_{2.5}$ presents

challenges due to the nature of EPA-reported PM$_{2.5}$ measurements in the AirNow database. These values are directly obtained through instrumental measurements, classifying any particle smaller than 2.5 micrograms as a PM$_{2.5}$ species. This method doesn't provide a clear means of distinguishing between the various particles detected by these instruments. In contrast, the PM$_{2.5}$ species in our study are defined based on CAMx model documentation (Ramboll Environment and Health, 2020). This divergence in approach makes a comprehensive PM$_{2.5}$ evaluation challenging and pursuing alternative assessment methods falls beyond the scope of our current study.
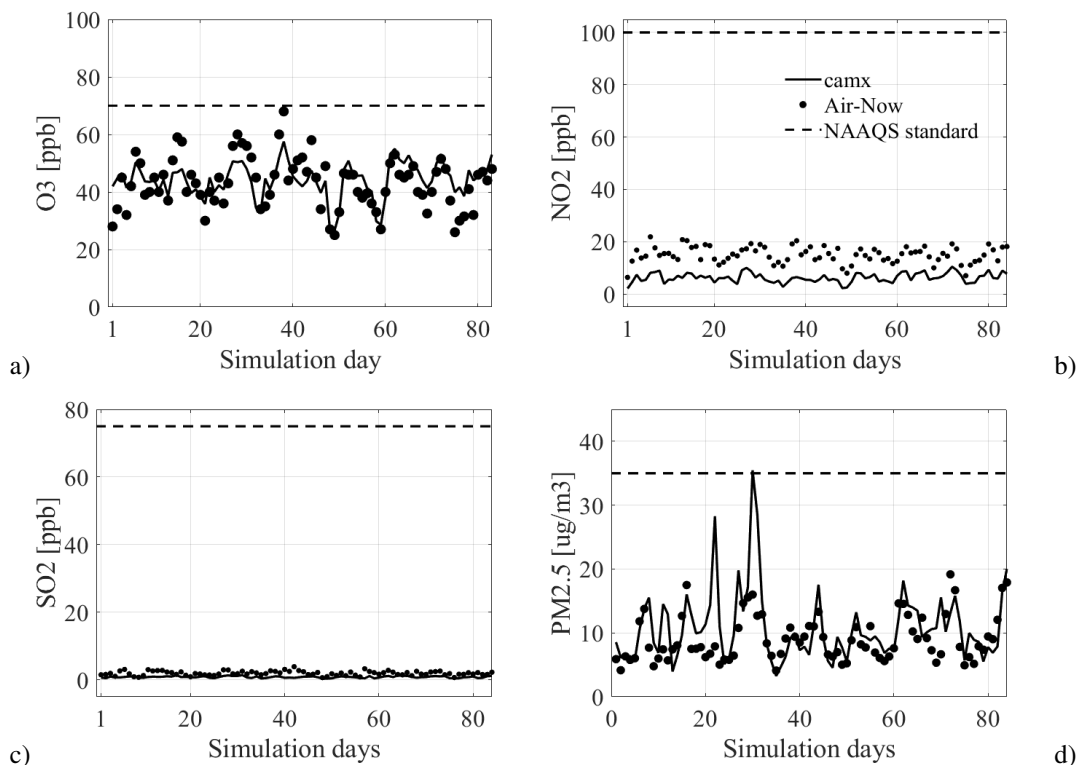
Figure 3. Model bias time series; CAMx model performance evaluated against the AirNow measurements; MBE is calculated across all stations at each day a) O$_3$ [ppb], b) NO$_2$ [ppb], and c) SO$_2$ [ppb], and d) $PM_{2.5}$ [$\mu g/m^3$]

Figure 3 illustrates the time series of the AirNow measurements across the simulation days (in black circles), as well as the co-located CAMx outputs for the pollutant of interest in the solid black line. The co-located data are such that they are extracted at the same hour as observations and at the mass point of the grid cell that contains that specific station. Figure 4, on the other hand, illustrates the mean bias error (MBE) calculated at every station and depicts a spatial distribution of the model MBE for each pollutant using the co-located data. CAMx demonstrates a tendency to slightly under- or over-estimate O$_3$ concentrations closer to the coast, and away from the coast, respectively (Figure 4a). Our focus is mainly on locations closer to the coast since that is where we detect the highest impact of shipping emissions. For O$_3$, a calculated MBE of -1.12 ppb indicates a systematic underestimation of around 2.5% across all monitoring stations within the designated domain. Overall, the model effectively

captures the O$_3$ trend and demonstrates a satisfactory level of agreement with observational data, as illustrated in Figure 3a. In addition, CAMx showcases a strong alignment with observational data in terms of SO$_2$ simulations with minimal deviation from the observations.

195   For PM$_{2.5}$, the model typically underestimates high PM$_{2.5}$ episodes, as is commonly observed in prior studies (Delle Monache et al., 2020; Golbazi et al., 2023). Nonetheless, for the remainder of the time, it demonstrates a strong alignment with observed data, as shown in Figure 3d. Figure 2d reveals that the model bias for PM$_{2.5}$ consistently remains below 5 μg/m3 for the majority of coastal stations, with only a few exceptions.

Shifting focus to NO$_2$, the model systematically underestimates NO$_2$ concentrations (Figure 3b, and Figure 4b). This
200   observation aligns with findings reported in existing literature (Ma et al., 2006). The notable underestimation of NO$_2$ levels within the model can be attributed to the fact that the monitoring stations are typically situated in close proximity to major roadways characterized by heavy traffic flow, resulting in elevated NO$_2$ emissions. Conversely, NO$_2$ concentrations at locations farther away from these monitoring stations tend to be significantly lower than those recorded by the sensors near high-traffic roads (Figure 2a). On the other hand, in the CAMx model, data is extracted from the nearest central mass point within a grid
205   cell containing the AirNow station's location, providing an averaged representation of NO$_2$ levels within that specific grid cell. Consequently, the inherent positive bias in observations contributes to the model's tendency to underestimate this pollutant.

Figure 4. CAMx model performance against the AirNow observations; MBE calculated at each station for a) O$_3$ [ppb], b) NO$_2$ [ppb], c) SO$_2$ [ppb], and d) PM$_{2.5}$ [$\mu g/m^3$]. Blue shades show a systematic underestimation, while the red shades illustrate a systematic overestimation by the model.

4 Results and discussion

We study the impacts of ship emissions on the concentrations of four criteria pollutants: $PM_{2.5}$, SO_2, NO_2, and O_3. We calculate the time-average concentrations over different time periods depending on the pollutant as follows, to match the EPA national standards: one hour for SO_2 and NO_2; 8 hours for O_3; and 24 hours for $PM_{2.5}$. We analyze every pollutant from two perspectives: 1) from a regulatory perspective, thus calculating the statistics that are as close as possible to the EPA design value for each pollutant (Table 2), and 2) from a worst-case perspective, thus calculating the maximum contribution of ships to each pollutant over the entire three-month study period.

Table 2. Design values for criteria pollutants (U.S. Environmental Protection Agency (EPA), 2022b). For attainment purposes, the design values should be calculated by taking the average of the various percentiles over the past three years; since only one year was simulated in this study, the 3-year average could not be calculated and therefore only the actual percentiles were used.

Pollutant	Design value	Threshold for attainment
O_3	4-th highest 8-hr averaged daily maximum	70 ppb
SO_2	99-th percentile 1-hr daily maximum	75 ppb
NO_2	98-th percentile 1-hr daily maximum	100 ppb
$PM_{2.5}$	98-th percentile 24-hr average	$35\,\mu g\,m^{-3}$

To calculate the maximum contribution, we first find the differences between the two cases (WithShips minus NoShips) at every grid cell, averaged over the relevant time interval, which depends on the pollutant (Table 2); then, we find the maximum difference through the 3 months at every grid cell as follows:

$$\max(\Delta P_{i,j}) = \max_{t \in [1...n]} (P_{i,j}^{WithShips}(t) - P_{i,j}^{NoShips}(t)) \tag{1}$$

where n is the number of data on the 1-, 8-, or 24-hr averaged pollutant P concentration values (the exact time averaging window depends on the pollutant, see Table 2) over the 3-month period of study, $P^{WithShips}$ and $P^{NoShips}$ are pollutant P concentrations with and without the ships, respectively, and i and j correspond to the model grid cell indices.

Although the maximum contribution from Eq. 1 is not valuable in terms of reaching or maintaining the EPA attainment for states, it is essential to understand the importance of maritime shipping on air quality, physically and statistically. A summary of the design values defined here for each pollutant to represent the EPA standards and the threshold for attainment are presented in Table 2. The defined design values follow the same criteria as defined by the EPA (U.S. Environmental Protection Agency (EPA), 2022b) but only for the time period of this study. For the remainder of the article, we will assume that the design values defined in Table 2 serve the purpose of analyzing the pollution from a regulatory perspective and are the same as the EPA standards for those pollutants for the time period of this study.

We find that the concentration of carbon monoxide (CO) remains unchanged in the presence of ships (not shown), suggesting that the CMV sector has minimal impact on the CO concentrations in the region. As such, we do not discuss the CO results in the rest of this study.

4.1 Fine particulate matter (PM$_{2.5}$)

The PM$_{2.5}$ species used in this study are those included in the CAMx model output (Ramboll Environment and Health, 2020). The EPA requires that the 3-year average of the 98-th percentile of the daily mean PM$_{2.5}$ concentrations should not exceed $35\,\mu g\,m^{-3}$. Here, we calculated the 98-th percentile of the 24-h averaged PM$_{2.5}$ concentrations at every grid cell during the simulation period in both scenarios, WithShips, and NoShips.

We find that PM$_{2.5}$ levels stayed below $35\,\mu g\,m^{-3}$ across most of the domain and that only two locations, i.e., Manhattan, NY, and Easton, PA (Figure 5a), crossed the $35\,\mu g\,m^{-3}$ maximum allowed concentrations and therefore were in non-attainment based on the design value defined in this study in Table 2. From a policy perspective, the CMV sector increases PM$_{2.5}$ levels up to $3.2\,\mu g\,m^{-3}$ in Manhattan, NY, and up to $2\,\mu g\,m^{-3}$ elsewhere (Figure 5c). This is while the percent contribution to PM$_{2.5}$ concentrations remains below 27% across the domain (Figure 5d). In a worst-case scenario, however, the maximum contribution of the ships to PM$_{2.5}$ concentrations within the 3 months is significantly high across the domain but due to the dominant southwesterly wind direction in the region (Golbazi et al., 2022), it mostly remains over the Atlantic Ocean (Figure 5b). The maximum impact on PM$_{2.5}$ during the 3 months reaches as high as $8\,\mu g\,m^{-3}$. Across the domain, the highest impacts are found offshore of MD and VA and in the Chesapeake Bay, DE. Over the land, the highest impacts are in Manhattan, NY, CT, and coastal MA.
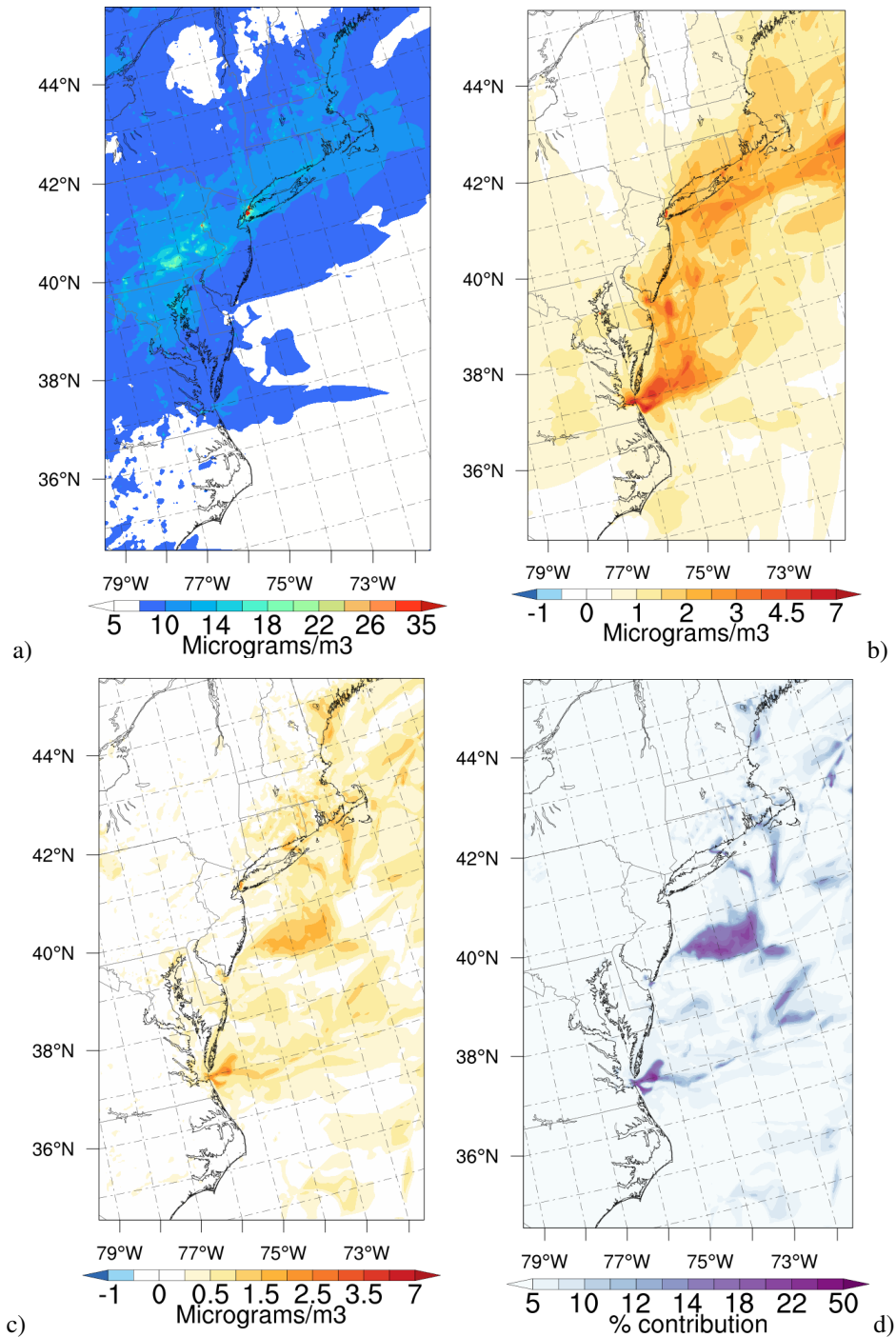
Figure 5. PM$_{2.5}$ concentration results: a) 98-th percentile of the 24-hr average PM$_{2.5}$ concentrations with ships (withShips); b) maximum contribution of the ships during the 3-month period (Eq. 1); c) difference between the two scenarios (WithShips minus NoShips) from a regulatory perspective, meaning the changes to the 98-th percentile PM$_{2.5}$ concentrations; and d) percent contribution of the ships to 98-th percentile of the 24-hr average PM$_{2.5}$ concentrations.

4.2 Sulfur dioxide (SO_2)

The SO_2 design value is defined as the 99-th percentile daily maximum SO_2 concentrations in the simulation period, which should not exceed 75 ppb (Table 2). Here we calculated the 99-th percentile of daily maximum SO_2 concentrations at every grid cell over the simulation period in the two scenarios, i.e., WithShips and NoShips. Then, we subtracted these two cases from one other (WithShips minus NoShips) to obtain the net effect of the maritime shipping sector.

Our results show that ships have a significantly high impact on SO_2 concentrations, up to 95% and 90% over the Atlantic Ocean and inland, respectively (Figure 6d). This suggests that the CMV sector is one of the highest contributors to SO_2 levels in the region. The increase in the SO_2 design value by ships remains mainly offshore and around the major shipping routes (Figure 6c). However, it reaches the interior of land in major ports and some parts of the coastal states. Over the simulation period, the contribution of the ships to the 99-th percentile daily SO_2 maxima is up to 45 ppb, with the highest impact in Baltimore, Maryland (MD), and Norfolk, Virginia (VA), and parts of New Jersey and Long Island (Figure 6c). We note that, however, the SO_2 design value in the region remained below 75 ppb in all states (Figure 6a). It is worth mentioning that the locations with the highest SO_2 concentrations are the ones highly impacted by the ships.

In addition, we calculated the 3-month maximum contributions of the ships to SO_2 concentrations, which indicates the worst-case scenario at every grid cell (figure 6b). Although the increase in SO_2 design value was mainly offshore, the maximum contribution of the ships to SO_2 showed a different pattern, with a maximum increase of up to ~185 ppb at a few grid cells around Norfolk, VA. We note that an occasional and short-term spike of high concentrations of SO_2, as we report here for Norfolk, is not necessarily associated with a strong health impact.
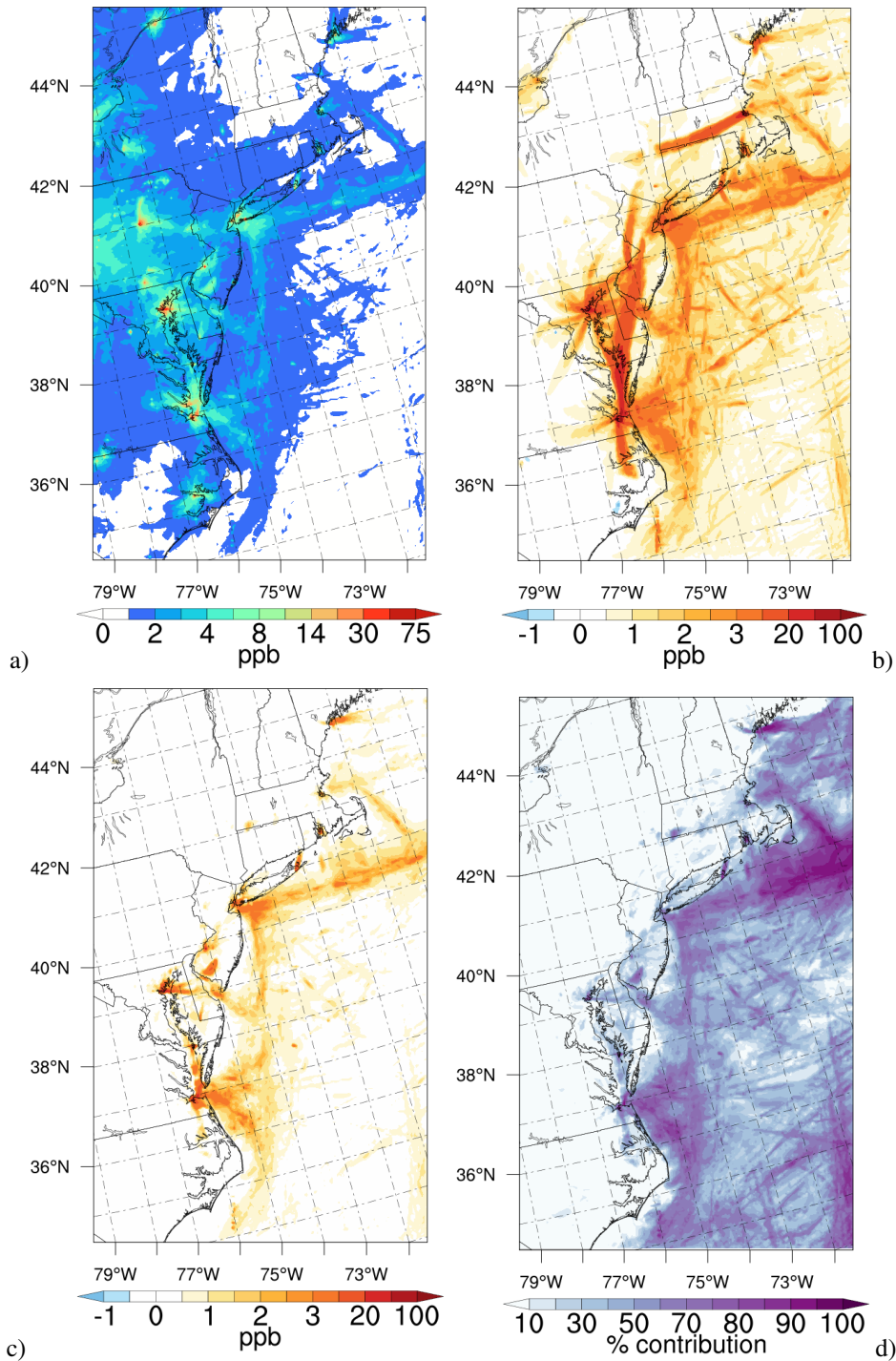
Figure 6. SO$_2$ concentration results: a) 99-th percentile of daily 1-hour maximum SO$_2$ concentrations with ships (WithShips); b) maximum contribution of the ships during the simulation period (Eq. 1); c) differences between the 99-th percentile daily maximum between the two scenarios (WithShips minus NoShips); and d) percent contribution of the ships to the 99-th percentile of the daily SO$_2$ maximum.

4.3 Nitrogen dioxide (NO$_2$)

NO_2 is a precursor to tropospheric ozone (O$_3$) formation, which has further negative impacts on human health (, EPA). NO$_2$ is generally directly emitted into the atmosphere from emission sources, including ships. We find that ships cause a significant increase in the 98-th percentile of daily maximum NO$_2$ concentrations, up to 34 ppb, but only at a few locations along the coast and in coastal states with major ports (Figure 7c), suggesting that, except for states with large ports, ships do not significantly impact the state compliance with the EPA standards. However, in NC, VA, DE, NY, and CT the shipping impacts reach beyond 15 ppb from a regulatory standpoint. Among these states, while NC remains in attainment with regulations (below 100 ppb), it experiences up to 80% contribution from the ships to its NO$_2$ concentrations. On the other hand, NY is the only state in the study domain that exceeds the 100 ppb standard for NO$_2$ concentrations, and shipping contribution to its non-attainment is 20-25%.

The maximum contribution of the ships to NO$_2$ concentrations, which is illustrated in Figure 7b, shows that, in a worst-case scenario, ships contributed to up to ~50 ppb of NO$_2$ along the coast and 75 ppb over the Atlantic, which is significantly high compared to 100 ppb standard. The 3-month highest impact happens near the major ports and shipping routes but stretches to the land and over the ocean.

4.4 Ozone (O$_3$)

Tropospheric ozone is formed by both naturally occurring and anthropogenic sources. Ozone is not emitted directly into the air, but, in the presence of sunlight, it is created by its precursors: VOC and NO$_x$. The rate of ozone production can be limited by either VOCs or NO$_x$. As a result, a specific location can be either VOC-limited or NO$_x$-limited. The rate of production/destruction of O$_3$ in the atmosphere is different in either of these regimes. We will further discuss this matter later in this section.

We use 8-hour average ozone concentrations for our analysis to maintain consistency with the EPA standards (U.S. Environmental Protection Agency (EPA), 2022b). We calculated the 8-hr averaged ozone values by averaging consecutive eight hours of O$_3$ outputs at each hour of the day and storing it at the start hour (Cohen et al., 1999). For instance, O$_3$ at 11:00 in a day indicates the time-averaged O$_3$ concentrations between hours 11:00 and 19:00 in that day. Hereafter, we will refer to the 8-hr averaged O$_3$ concentrations simply as O$_3$ concentrations.

Ambient ozone concentrations are directly affected by temperature, solar radiation, wind speed, and other meteorological factors. Since O$_3$ production is a photochemical reaction, its peak concentrations are found during the daytime when tropospheric ultraviolet radiation in the atmosphere is highest. Since the focus of this study is the daily high episodes of O$_3$ that are associated with adverse health impacts, we limit our analysis of the maximum impacts to only daytime hours. To select the daytime hours, we considered the 8-hr averaged O$_3$ daily profiles in 10 different locations along the coast from which 4 selected locations are shown in Figure 8. The lowest concentrations of O$_3$ are associated with hours 00:00 to 08:00 UTC (20:00 to 04:00 local time). We eliminated these hours from our analysis to only focus on concentrations during the high episodes. Therefore, we select the hours with peak O$_3$ concentrations during the 24-h period i.e., 09:00 to 23:00 UTC (05:00 to 19:00 local time).
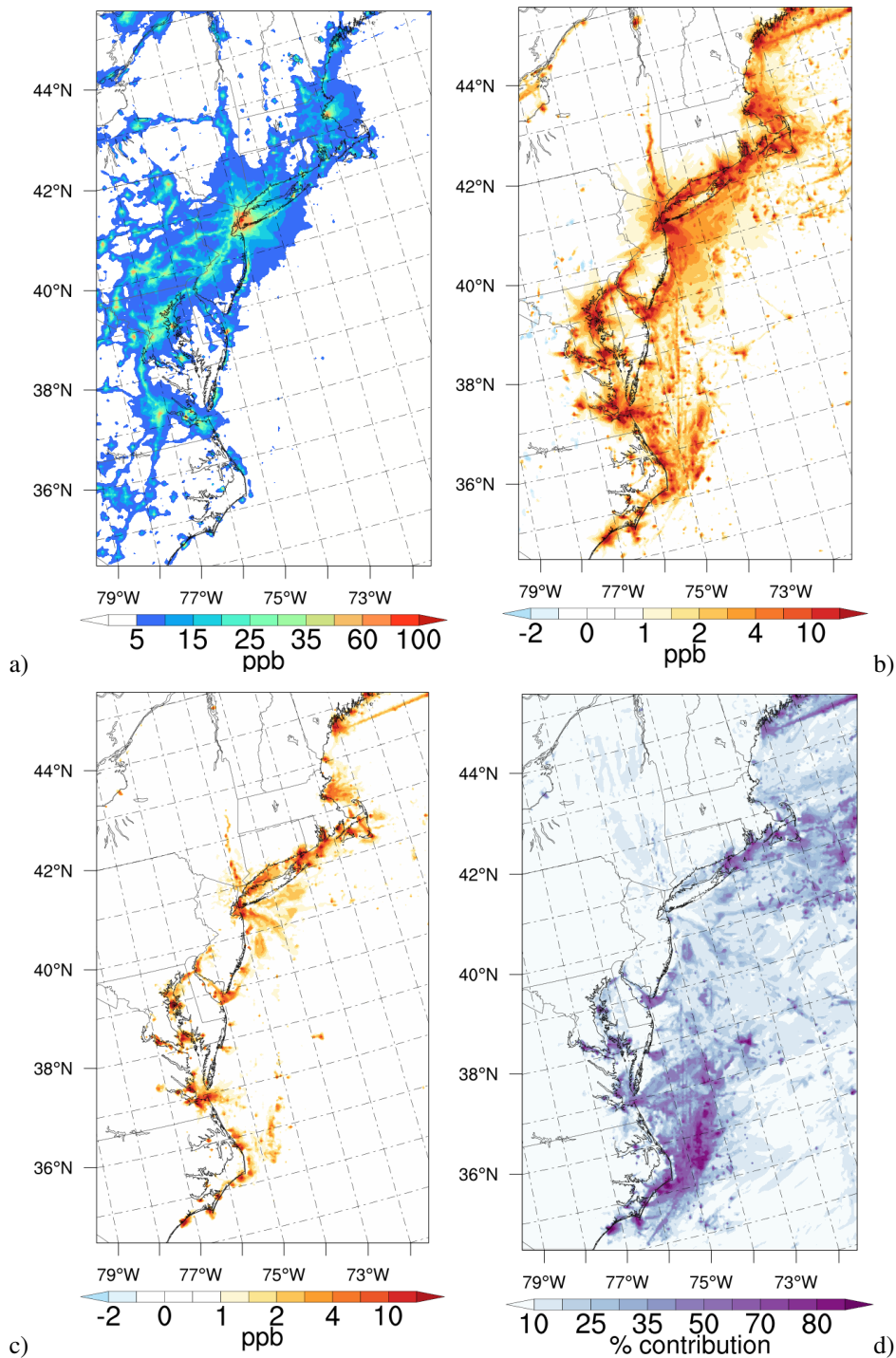
Figure 7. NO$_2$ concentration results: a) 98-th percentile of 1-hour daily maximum NO$_2$ concentrations with ships (WithShips); b) maximum contribution of the ships during the simulation period (Eq. 1); c) differences between the 98-th percentile of the 1-hour daily maximum between the two scenarios (WithShips minus NoShips); and d) percent contribution of the ships to the 98-th percentile of the daily NO$_2$ maximum.

We find that although ship emissions contribute to O_3 enhancement in the region, they reduce O_3 at some urban locations. We detect a significant increase or decrease in O_3 concentrations in the presence of the ships, depending on whether the location was NO_x or VOC limited.
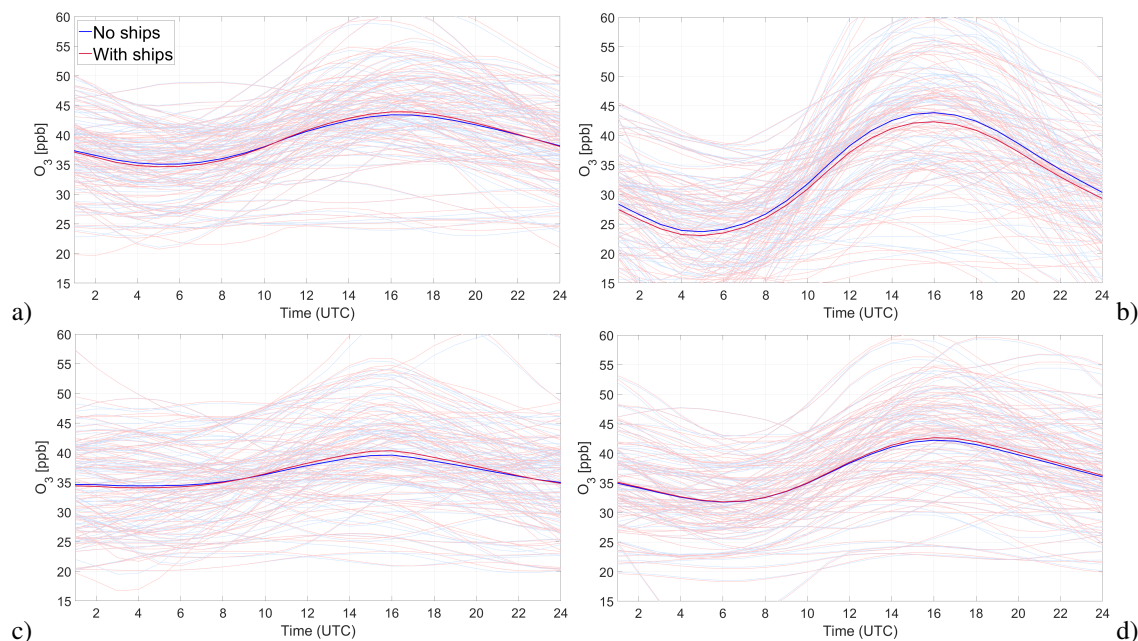
Figure 8. Eight-hour average O_3 concentration time series at four different locations along the East Coast from June 1st to August 30st, 2018: a) Atlantic City, NJ; b) Manhattan, NY; c) Cape Cod, MA; and d) Providence, RI. The thin lines represent the daily time series and the thick lines are the 3-month average profiles with red lines for WithShips and blue lines for the NoShips simulations.

The maximum contribution of the ships to the O_3 levels over the entire 3-month period is illustrated in Figure 9c as a worst-case scenario. Over the ocean, the maximum increase is large, up to 8.6 ppb. However, the pollution increase remained primarily offshore and did not significantly impact the coastal areas. O_3 increased by 4-5 ppb at most in parts of North Carolina, Baltimore, MD, and parts of CT, and MA. Otherwise, the maximum increase over the land was up to 3.5 ppb. It's important to note that the maximum impact is not necessarily at the time when high O_3 episodes (from a regulatory perspective) are found. Despite the O_3 increase over the Atlantic, at the shore where the major ports are built, the maximum contribution of the ships is negative, suggesting that O_3 was destructed in the presence of the ships. This is due to the complex nature of atmospheric chemistry, where the fresh NO emissions from the ships scavenge O_3 and reduce its concentrations in urban VOC-limited areas.

While Figure 9b is important to understand the worst-case scenario of the shipping impact on O_3 pollution in the region, it does not help to measure the impact of these changes on state compliance with EPA standards. This is because a high impact on O_3 in the worst-case scenario may not correspond to the time of the day when O_3 daily maxima occurred. Therefore, to study the impacts of ship emissions from a policy perspective, it is necessary to explore the impacts on the O_3 design value at every grid cell. For O_3, the EPA defines this standard as the 4-th highest 8-hr averaged O_3 daily maxima, averaged over a 3-year period
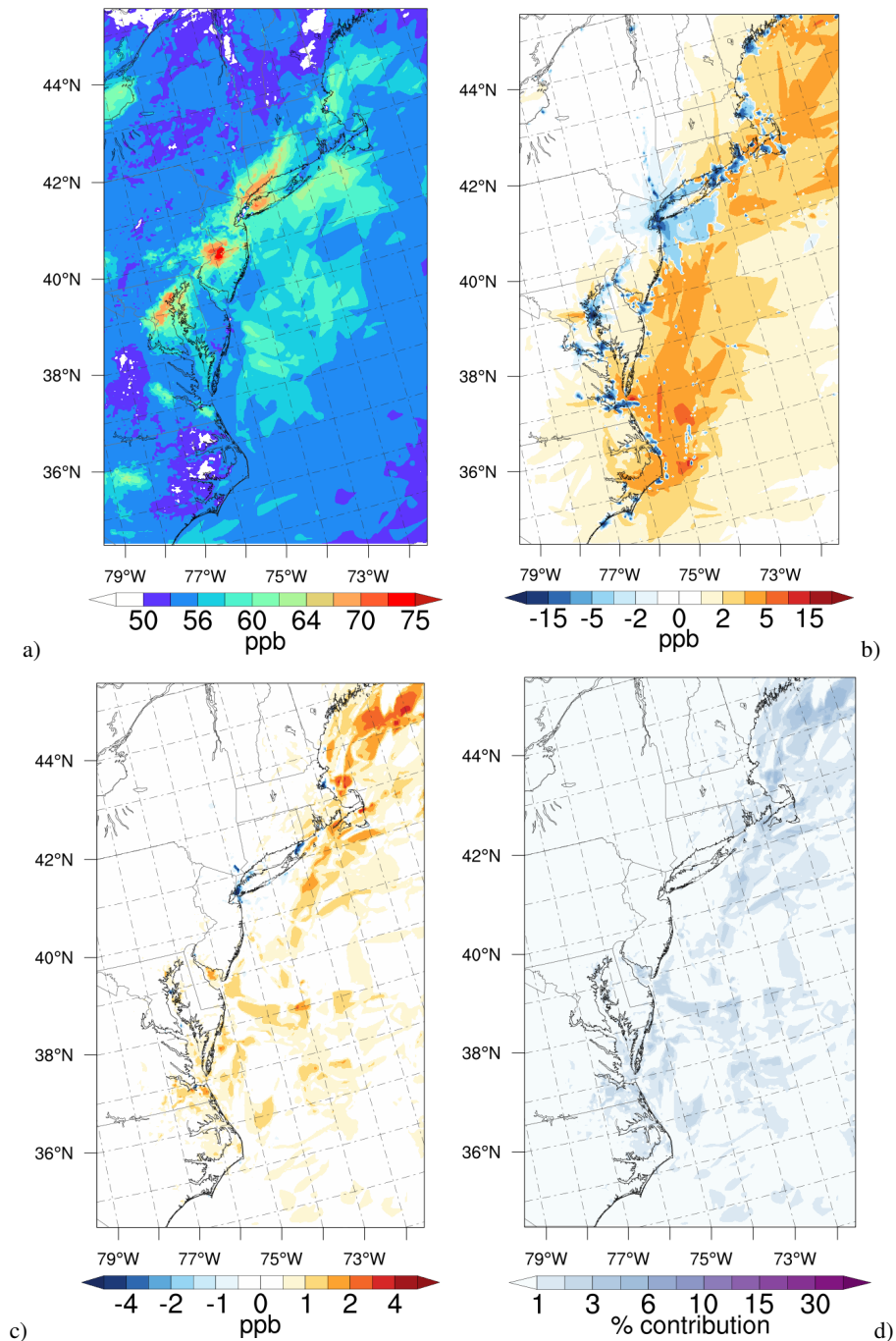
Figure 9. O_3 concentration results: a) 4-th highest 8-hour daily maximum O_3 concentrations with ships (WithShips); b) maximum contribution of the ships during the 3-month simulation period (Eq. 1); c) differences between the 4-th highest 8-hour daily maximum between the two scenarios (WithShips minus NoShips); and d) percent contribution of the ships to the 4-th highest daily O_3 maximum.

which should not exceed 70 ppb (U.S. Environmental Protection Agency (EPA), 2022b). Since we do not have data for three consecutive years, we focus on the 4-th highest daily maximum in our study period, the summer of 2018. Hereafter, we will refer to this value as O_3 design value in this study. We assume that this value represents the 4th highest daily maximum in the year 2018 since the highest O_3 episodes are expected to occur during the summer period. Thus, the regions with higher than 70 ppb O_3 concentrations in 9a are most susceptible to being in non-attainment with the EPA standards and therefore the impacts of the ships are of higher significance in those regions. Out of all states in the domain, NY, NJ, and MD are the only states that exceed the 70 ppb standard and are likely to be in non-attainment. All other states stay in attainment with the standards defined in Table 2 in either scenario.

From a policy perspective, O_3 design values increased in presence of the ships by up to 3.5 over the Atlantic Ocean. However, we find a reduction (up to 6.5 ppb) in O_3 concentrations at major ports along the East Coast (Figure 9c), where fresh NO is emitted by the ships into the atmosphere in VOC-limited regions (Figure 10). In most parts, the major impact of the ships remains offshore away from the coastal areas. However, in some regions in MA, RI, CT, ME, VA, NC, and MD ships contribute to O_3 increase at the coast from which, only MD is likely to be in non-attainment. The highest increase in O_3 design value inland is found in VA and NC and is up to 2.5 ppb, while we note that in NY, the 4-th highest daily maximum is decreased by 4 ppb in presence of the ships for the reasons discussed later in this section. However, the decrease in O_3 values remains in Manhattan, NY, and is not associated with the parts of Long Island (NY) where O_3 exceeds the standards.

In the atmosphere, the formation or destruction of ozone depends on the concentrations of both NO_x and VOC and the ratio between them (VOC/NOx). Transportation usually is associated with high NO_x emissions, therefore O_3 is generally NO_x-limited in rural areas and VOC-limited in urban areas, with low and high traffic densities, respectively.

In the VOC-limited regions, high concentrations of freshly emitted NO locally scavenge O_3 and lead to the formation of NO_2. Close to the emission sources, this titration process can be considered an ozone sink. In addition, high NO_2 concentrations deflect the initial oxidation step of VOC by forming other products such as nitric acid (HNO_3), which slows down the formation of O_3 (National Research Council, 1992; Beck et al., 1998). Because of these reactions, an increase in NO leads to a decrease in O_3 at VOC-limitted regions.

In CAMx, the VOC-limited regime is defined when the rate of change of hydrogen peroxide (H_2O_2) is lower compared to the rate of change of HNO_3. A higher $\Delta H_2O_2/\Delta HNO_3$ ratio indicates a NO_x-limited regime, while a lower $\Delta H_2O_2/\Delta HNO_3$ ratio corresponds to a VOC-limited regime. There are other indicators for determining the NO_x/VOC-limited regimes that are discussed in the literature (Li et al., 2022). However, here we use the $\Delta H_2O_2/\Delta HNO_3$ ratio as is used in the CAMx model (Ramboll Environment and Health, 2020).

To understand the formation/destruction of ozone in the presence of the ships in our study domain, we calculated the frequency of the VOC-limited regime based on the ratio at every grid cell. Figure 10a illustrates the percentage of the times that a VOC-limited regime occurred at every cell, which is the highest along the coast and in major cities. This indicates that O_3 may be affected by titration when ship emissions are present. We find that the NO concentrations increase along the coast where we detect a decrease in O_3 concentrations (Figure 10b) and a VOC-limited regime (Figure 10c).

This finding does not necessarily mean that ships help create better air quality since a reduction in O_3 is due to a significant increase in other important air pollutants i.e., NO_x concentrations.
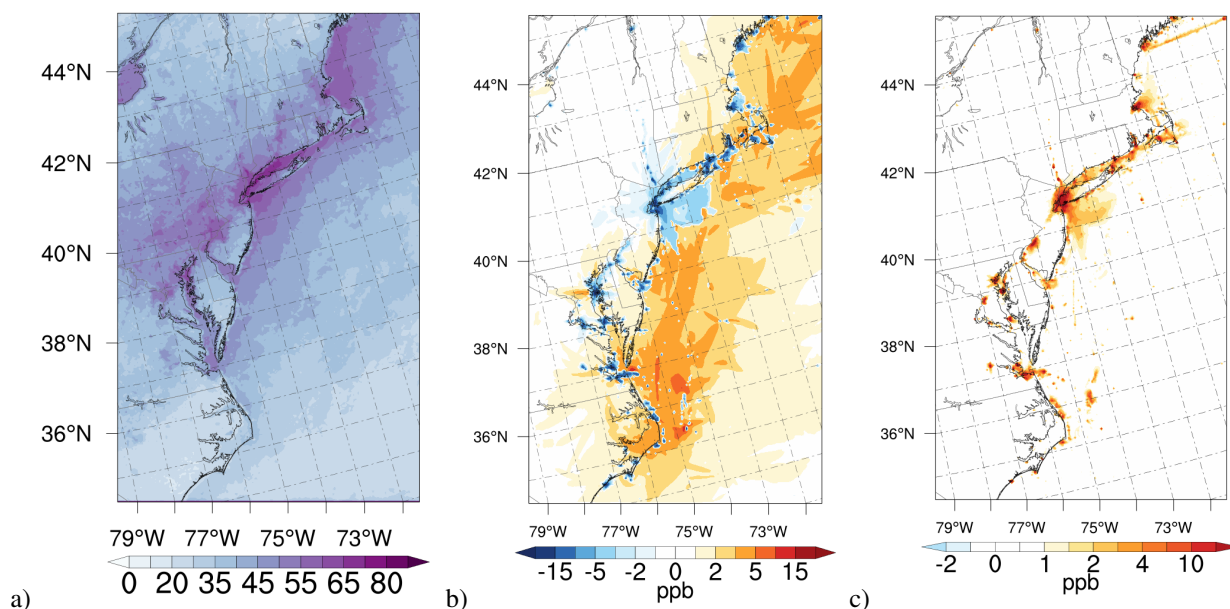
Figure 10. VOC- versus NO_x-limited regime determination: a) percentage of the times when $\Delta H_2O_2/\Delta HNO_3 < 0.35$ as determined in CAMx model, which is an indication of a VOC-limited regime; b) maximum contribution of ships to O_3 pollution (Figure 9c); and c) same as in b) but for NO.

4.5 Diurnal Cycle of the impacts

In order to examine the diurnal variations in the impact of shipping activities on each of the four pollutants, we generated time series data representing the daily cycles of changes induced by ships. To achieve this, we specifically chose four key locations along the eastern coast: Manhattan, New York; Baltimore, Maryland; Boston, Massachusetts; and Norfolk, Virginia. This selection was deliberate, as these locations encompass large cities as well as major ports, making them suitable representatives for assessing the shipping-related effects on air quality.

350

Figure 11. Diurnal cycle of the ship emission impacts on pollutants for a) SO_2 [ppb], b) NO_2 [ppb], c) O_3 [ppb], d) $PM_{2.5}$ [$\mu g/m^3$]. The first through fourth columns represent changes in Manhattan, NY, Baltimore, MD, Boston, MA, and Norfolk, VA, respectively.

The dashed lines are the 25th and 75th percentiles, offering insights into the distribution of the impacts across various days
355 and stations at each simulation hour. In contrast, the solid pink line represents the median impact attributed to the presence of ships. For both NO_2 and SO_2, we observe an increase in concentrations when ships are present at all hours, as evidenced by the positive values of the median diurnal impact. Notably, the most significant impact for NO_2 is observed around 05:00 – 15:00 UTC (corresponding to 01:00 to 11:00 local time). For SO_2, we do not detect a clear diurnal pattern across all four locations. The median changes in O_3 levels show varying patterns across different locations. In Baltimore, MD, and Norfolk, VA, the
360 median impacts on O_3 are minimal. In Manhattan, NY, O_3 levels demonstrate consistent negative changes across all hours, indicating a reduction in O_3 concentration in the presence of ships, with the most pronounced decrease occurring between 05:00 - 12:00 UTC (equivalent to 01:00 - 08:00 local time). It's important to note that these values represent the 8-hour average O_3 concentrations, meaning that, for instance, 08:00 local time represents the average O_3 levels between hours 08:00 and 16:00. Conversely, in Boston, MA, the most significant impacts of ships on O_3 levels are observed between 11:00 and 20:00 UTC
365 (equivalent to 07:00 - 16:00 local time) and are increased.

$PM_{2.5}$ shows a similar diurnal pattern to NO_2 as it shows a positive impact (increase in $PM_{2.5}$ levels by the ships) in all hours, with the highest impact during the   00:00 – 12:00 UTC (corresponding to   20:00 to 08:00 local time). Apart from Manhattan, NY, where the highest impacts occur around hour 20:00 UTC (16:00 local time).

It's worth highlighting that the influence of shipping emissions on the four pollutants shown in Figures 5–9 (b-c) may be different than the findings in Figure 11. This divergence arises from our utilization of distinct metrics in these two analyses. In Figure 11, we base our assessment on median impacts within the four locations, whereas in the other figures, we evaluate the impacts with regard to EPA regulations or under a worst-case scenario.

5 Conclusions

Ships emit significant amounts of pollutants within 400 km of the shores. Here, we studied the ocean-going ship emissions on the air quality of the U.S. East Coast. We utilized the WRF-CAMx modeling system to simulate the pollution concentrations in the presence and absence of shipping activities along the East Coast and at the major ports. We used the WRF model to provide the meteorological inputs for the CAMx air quality model for the year 2018, on which the most recent EPA/NEI emission inventory is based. We particularly focused on $PM_{2.5}$, SO_2, NO_2, and O_3. Overall, we studied the outcomes of every pollutant from two perspectives: 1) from the EPA perspective concerning the national concentration standards for each specific pollutant, and 2) the maximum contribution of ships to that pollutant over the 3 months. Our assessment of the CAMx model's performance reveals strong performance in simulating SO_2 levels. The model shows a slight underestimation of O_3 concentrations near the coast and a slight overestimation farther from the shore. Nevertheless, the mean bias error for O_3 is limited to -1.12 ppb. Likewise, the bias in $PM_{2.5}$ concentrations remains below 5 $\mu g/m^3$. On the other hand, the model exhibits a noticeable underestimation of NO_2 concentrations, primarily stemming from a positive bias in observations collected in proximity to major roads.

We find that shipping increases the $PM_{2.5}$ concentrations across the domain. the 98-th percentile daily average $PM_{2.5}$ levels increased by 3.2 $\mu g\,m^{-3}$ over the ocean and in some coastal areas. However, in a worst-case scenario, ships contribute up to approximately 8.0 $\mu g\,m^{-3}$ to $PM_{2.5}$ concentrations, only over the Atlantic off the coast of MD, and VA. In addition, we find that ships have a significantly high impact, up to 95% and 90%, on the SO_2 concentrations over the Atlantic and inland, respectively. This suggests that the CMV sector is one of the highest contributors to SO_2 levels in the region. The shipping contribution to SO_2 levels was up to 45 ppb over coastal regions. Ship emissions also impacted the NO_2 design value by up to 34 ppb. In addition, our simulation results show that the impact of ship emissions on O_3 concentrations is not uniform, meaning that maritime shipping affects ozone pollution in both positive and negative ways. Although over the ocean O_3 concentrations increase significantly in the presence of ships (up to 8.6 ppb), in coastal areas with major cities and major ports O_3 concentrations decrease by up to ~6.5 ppb. To understand the reasons behind the O_3 reduction in the presence of ships, we analyzed the $\Delta H_2O_2/\Delta HNO_3$ ratio in the region, which is used to determine NO_x- or VOC-limited ozone production, as well as changes to NO concentrations, since they play a significant role in O_3 formation and destruction. We found that ships emit significant amounts of fresh NO in the atmosphere, which then helps scavenge O_3 in VOC-limited regimes. As a result, with higher NO concentrations in the atmosphere produced by ship emissions, O_3 is destructed in major cities and urban areas. By contrast, over the ocean (a NO_x-limited regime), excessive NO_x emissions due to the ships contribute to the formation of O_3 and therefore an enhancement in O_3 concentrations. It is important to note that the destruction of O_3 by ship emissions in major cities does not necessarily mean that the ships create better air quality because a decrease in O_3 is a consequence of a significant increase in other pollutants

like NO. The diurnal cycle in the impact of shipping emissions across four major cities shows different patterns for different locations. For instance, the highest impacts on O3, occur at different times for different locations. $PM_{2.5}$ and NO_2, however, experience the highest changes in the early morning in most locations. On the other hand, we do not detect consistent patterns for changes in SO_2.

Overall, the majority of the time, due to the dominant southwesterly wind direction in the region, the impacts on different pollutants remained spatially confined offshore. However, in some coastal areas near the major ports, the impacts were significant.

Data availability

The data for the model setup is available in the GitHub repository at:

https://github.com/golbazimaryam/ShippingEmissionsAndAirQuality

Author contribution

M. Golbazi contributed to the design of the study, preparing the manuscript, setting up and carrying out simulations, and analysis. C.L. Archer contributed to the design of the project, preparing the manuscript and editing, as well as data analysis.

Competing interests

"The authors declare that they have no conflict of interest."

Acknowledgements. *

Partial funding for this research came from the University of Delaware (UD) Graduate College Doctoral Fellowship and from the Delaware Natural Resources and Environmental Control (DNREC, award no. 18A00378). The simulations were conducted on the UD Caviness and NCAR Cheyenne high-performance computer clusters.

420 **References**

Aksoyoglu, S., Baltensperger, U., and Prévôt, A. S.: Contribution of ship emissions to the concentration and deposition of air pollutants in
    Europe, Atmospheric Chemistry and Physics, 16, 1895–1906, 2016.

Ancell, B. C., Bogusz, A., Lauridsen, M. J., and Nauert, C. J.: Seeding Chaos: The Dire Consequences of Numerical Noise in NWP
    Perturbation Experiments, Bulletin of the American Meteorological Society, 99, 615 – 628, https://doi.org/10.1175/BAMS-D-17-0129.1,
425   2018.

Archer, C. L., Colle, B. A., Veron, D. L., Veron, F., and Sienkiewicz, M. J.: On the predominance of unstable atmospheric conditions in the
    marine boundary layer offshore of the US northeastern coast, Journal of Geophysical Research: Atmospheres, 121, 8869–8885, 2016.

Archer, C. L., Cervone, G., Golbazi, M., Al Fahel, N., and Hultquist, C.: Changes in air quality and human mobility in the USA during the
    COVID-19 pandemic, Bulletin of Atmospheric Science and Technology, 1, 491–514, 2020.

430 Arya, S. P. et al.: Air pollution meteorology and dispersion, vol. 310, Oxford University Press New York, 1999.

Beck, J., Krzyzanowski, M., and Koffi, B.: Tropospheric Ozone in the European Union - The consolidated report, Tech. rep., EEA Topic
    Report, 1998.

Cohen, J., Fitz-Simons, T., and Wayland, M.: Guideline on data handling conventions for the PM NAAQS, Tech. rep., Environmental Protection
    Agency, Office of Air Quality Planning and . . . , 1999.

435 Corbett, J. J. and Fischbeck, P.: Emissions from ships, Science, 278, 823–824, 1997.

Corbett, J. J. and Köhler, H. W.: Updated emissions from ocean shipping., Journal of Geophysical Research, 108, 2003.

Corbett, J. J., Fischbeck, P. S., and Pandis, S. N.: Global nitrogen and sulfur inventories for oceangoing ships, Journal of Geophysical Research:
    Atmospheres, 104, 3457–3470, 1999.

Corbett, J. J., Winebrake, J. J., Green, E. H., Kasibhatla, P., Eyring, V., and Lauer, A.: Mortality from ship emissions: a global assessment,
440   Environmental science & technology, 41, 8512–8518, 2007.

Delle Monache, L., Alessandrini, S., Djalalova, I., Wilczak, J., Knievel, J. C., and Kumar, R.: Improving air quality predictions over the
    United States with an analog ensemble, Weather and Forecasting, 35, 2145–2162, 2020.

Endresen, O., Sorgard, E., Sundet, J., Dalsoren, S., Isaksen, I., Berglen, T., and Gravir, G.: Emission from international sea transportation
    and environmental impact., Journal of Geophysical Research, 108, 2003.

445 Endresen, O., Sorgard, E., Behrens, H. L., Brett, P. O., and Isaksen, I. S. A.: A historical reconstruction of ships fuel consumption and
    emissions., Journal of Geophysical Research, 112, 2007.

(EPA), U. E. P. A.: Ground-level ozone pollution, https://www.epa.gov/no2-pollution/basic-information-about-no2#WhatisNO2, 2020.

Eyring, V.: Updated Study on Greenhouse Gas Emissions from Ships: Climate Impacts, Tech. rep., 2008.

Eyring, V., Köhler, H., Van Aardenne, J., and Lauer, A.: Emissions from international shipping: 1. The last 50 years, Journal of Geophysical
450   Research: Atmospheres, 110, 2005.

Eyring, V., Corbett, J. J., Lee, D. S., and Winebrake, J. J.: Brief summary of the impact of ship emissions on atmospheric composition,
    climate, and human health, Tech. rep., Health and Environment sub-group of the International Maritime Organization, 2007a.

Eyring, V., Stevenson, D. S., Lauer, A., Dentener, F. J., Butler, T., Collins, W. J., Ellingsen, K., Gauss, M., Hauglustaine, D. A., Isaksen,
    I. S., et al.: Multi-model simulations of the impact of international shipping on Atmospheric Chemistry and Climate in 2000 and 2030,
455   Atmospheric Chemistry and Physics, 7, 757–780, 2007b.

Eyring, V., Isaksen, I. S., Berntsen, T., Collins, W. J., Corbett, J. J., Endresen, O., Grainger, R. G., Moldanova, J., Schlager, H., and Stevenson, D. S.: Transport impacts on atmosphere and climate: Shipping, Atmospheric Environment, 44, 4735–4771, 2010a.

Eyring, V., Isaksen, I. S. A., Berntsen, T., Collins, W. J., Corbett, J. J., Endresen, O., Grainger, R. G., Moldanova, J., Schlager, H., and Stevenson, D. S.: Transport impacts on atmosphere and climate: Shipping, Atmospheric Environment, 44, 4735–4771, 2010b.

460   Finlayson-Pitts, B. and Pitts Jr, J.: Atmospheric chemistry of tropospheric ozone formation: scientific and regulatory implications, Air & Waste, 43, 1091–1100, 1993.

Foley, K. M., Hogrefe, C., Pouliot, G., Possiel, N., Roselle, S. J., Simon, H., and Timin, B.: Dynamic evaluation of CMAQ part I: Separating the effects of changing emissions and changing meteorology on ozone levels between 2002 and 2005 in the eastern US, Atmospheric Environment, 103, 247–255, 2015.

465   Fuller, R., Landrigan, P. J., Balakrishnan, K., Bathan, G., Bose-O'Reilly, S., Brauer, M., Caravanos, J., Chiles, T., Cohen, A., Corra, L., et al.: Pollution and health: a progress update, The Lancet Planetary Health, 2022.

Golbazi, M. and Archer, C. L.: Methods to Estimate Surface Roughness Length for Offshore Wind Energy, Advances in Meteorology, 2019.

Golbazi, M., Archer, C. L., and Alessandrini, S.: Surface impacts of large offshore wind farms, Environmental Research Letters, 17, 064 021, 2022.

470   Golbazi, M., Kumar, R., and Alessandrini, S.: Enhancing air quality forecasts across the contiguous United States (CONUS) during wildfires using an Analog-based post-processing methods, Tech. rep., Copernicus Meetings, 2023.

Kumar, R., Lee, J. A., Delle Monache, L., and Alessandrini, S.: Effect of meteorological variability on fine particulate matter simulations over the contiguous United States, Journal of Geophysical Research: Atmospheres, 124, 5669–5694, 2019.

Li, X., Qin, M., Li, L., Gong, K., Shen, H., Li, J., and Hu, J.: Examining the implications of photochemical indicators for O3–NOx–VOC
475   sensitivity and control strategies: A case study in the Yangtze River Delta (YRD), China, Atmospheric Chemistry and Physics, 22, 14 799–14 811, 2022.

Lin, J.-T. and McElroy, M. B.: Detection from space of a reduction in anthropogenic emissions of nitrogen oxides during the Chinese economic downturn, Atmospheric Chemistry and Physics, 2011.

Liu, H., Fu, M., Jin, X., Shang, Y., Shindell, D., Faluvegi, G., Shindell, C., and He, K.: Health and climate impacts of ocean-going vessels in
480   East Asia, Nature climate change, 6, 1037–1041, 2016.

Lv, Z., Liu, H., Ying, Q., Fu, M., Meng, Z., Wang, Y., Wei, W., Gong, H., and He, K.: Impacts of shipping emissions on PM 2.5 pollution in China, Atmospheric Chemistry and Physics, 18, 15 811–15 824, 2018.

Ma, J., Richter, A., Burrows, J. P., Nüß, H., and van Aardenne, J. A.: Comparison of model-simulated tropospheric NO2 over China with GOME-satellite data, Atmospheric Environment, 40, 593–604, 2006.

485   Moghani, M., Archer, C. L., and Mirzakhalili, A.: The importance of transport to ozone pollution in the U.S. Mid-Atlantic, Atmospheric Environment, 191, 420–431, 2018.

Murray, C. J. L. and Lopez, A. D.: Evidence-based health policy — Lessons from the Global Burden of Disease Study, Science, 274, 740–743, 1996.

National Research Council: Rethinking the ozone problem in urban and regional air pollution, National Academies Press, Washington, DC,
490   https://doi.org/10.17226/1889, 1992.

Niemeier, U., Granier, C., Kornblueh, L., Walters, S., and Brasseur, G.: Global impact of road traffic on atmospheric chemical composition and on ozone climate forcing., Journal of Geophysical Research: Atmospheres, 2006.

Ramboll Environment and Health: COMPREHENSIVE AIR QUALITY MODEL WITH EXTENSIONS Version 7.10 – User's guide, Tech. rep., https://camx-wp.azurewebsites.net/Files/CAMxUsersGuide_v7.10.pdf, 2020.

495 Ryu, Y.-H., Hodzic, A., Barre, J., Descombes, G., and Minnis, P.: Quantifying errors in surface ozone predictions associated with clouds over the CONUS: a WRF-Chem modeling study using<? xmltex\break?> satellite cloud retrievals, Atmospheric Chemistry and Physics, 18, 7509–7525, 2018.

Schnurr, R. E. and Walker, T. R.: Marine Transportation and Energy Use, in: Reference Module in Earth Systems and Environmental Sciences, Elsevier, 2019.

500 Seinfeld, J. H. and Pandis, S. N.: Atmospheric Chemistry and Physics, John Wiley and sons, 1998.

Serra, P. and Fancello, G.: Towards the IMO's GHG goals: A critical overview of the perspectives and challenges of the main options for decarbonizing international shipping, Sustainability, 12, 3220, 2020.

Skamarock, W. C., Klemp, J. B., Dudhia, J., Gill, D. O., Liu, Z., Berner, J., Wang, W., Powers, J. G., Duda, M. G., Barker, D. M., et al.: A description of the advanced research WRF model version 4, Tech. rep., National Center for Atmospheric Research, Boulder, CO, USA, 505 2019.

Smith, T. W., Jalkanen, J., Anderson, B., Corbett, J., Faber, J., Hanayama, S., O'keeffe, E., Parker, S., Johansson, L., Aldous, L., et al.: Third IMO greenhouse gas study 2014, 2015.

U.S. Environmental Protection Agency: 2020 National Emissions Inventory Technical Support Document: Commercial Marine Vessels, Tech. rep., https://www.epa.gov/system/files/documents/2023-03/NEI2020_TSD_Section11_CMV.pdf, 2020.

510 U.S. Environmental Protection Agency: 2017 National Emissions Inventory: January 2021 Updated Release, Technical Support Document, Tech. rep., https://www.epa.gov/air-emissions-inventories/2017-national-emissions-inventory-january-2021-updated-release-technical, 2021.

U.S. Environmental Protection Agency (EPA): PROFILE OF VERSION 1 OF THE 2014 NATIONAL EMISSIONS INVENTORY, Tech. rep., Office of Air Quality Planning and Standards, https://www.epa.gov/sites/production/files/2017-04/documents/2014neiv1_profile_ 515 final_april182017.pdf,Accessed06/17/2020, 2017.

U.S. Environmental Protection Agency (EPA): Nitrogen Dioxide (NO_2) Pollution, https://www.epa.gov/ground-level-ozone-pollution/ground-level-ozone-basics, accessed 07/28/2020, 2020a.

U.S. Environmental Protection Agency (EPA): Particulate Matter (PM) Pollution, https://www.epa.gov/pm-pollution/particulate-matter-pm-basics#PM, accessed 06/10/2020, 2020b.

520 U.S. Environmental Protection Agency (EPA): Photochemical Air Quality Modeling, Support Center for Regulatory Atmospheric Modeling (SCRAM), https://www.epa.gov/scram/photochemical-air-quality-modeling, accessed on 12/01/2022, 2022a.

U.S. Environmental Protection Agency (EPA): NAAQS Table, https://www.epa.gov/criteria-air-pollutants/naaqs-table, accessed 04/04/2022, 2022b.

Viana, M., Amato, F., Alastuey, A., Querol, X., Moreno, T., Garcia Dos Santos, S., Herce, M. D., and Fernández-Patier, R.: Chemical tracers 525 of particulate emissions from commercial shipping, Environmental science & technology, 43, 7472–7477, 2009.

Viana, M., Hammingh, P., Colette, A., Querol, X., Degraeuwe, B., Vlieger, I., and Aardenne, J.: Impact of maritime transport emissions on coastal air quality in Europe, Atmospheric Environment, 2014.

Wan, Z., Zhu, M., Chen, S., and Sperling, D.: Pollution: Three steps to a green shipping industry, Nature, 530, 275–277, 2016.

Yao, Z., Wu, B., Shen, X., Cao, X., Jiang, X., Ye, Y., and He, K.: On-road emission characteristics of VOCs from rural vehicles and their 530 ozone formation potential in Beijing, China., Atmospheric Environment, 2015.

Zhang, F., Bei, N., Nielsen-Gammon, J. W., Li, G., Zhang, R., Stuart, A., and Aksoy, A.: Impacts of meteorological uncertainties on ozone pollution predictability estimated through meteorological and photochemical ensemble forecasts, Journal of Geophysical Research: Atmospheres, 112, 2007.

Zhang, L., Jacob, D. J., Yue, X., Downey, N. V., Wood, D. A., and Blewitt, D.: Sources contributing to background surface ozone in the US Intermountain West., Atmospheric Chemistry and Physics, 2014.

535

Title: Impacts of maritime shipping on air pollution along the U.S. East Coast

paper rebuttal:

Reviewer #1:

This manuscript presented a modeling study of shipping emission impacts on air quality over east coast of the U.S. and reported significant impacts over some areas. Impacts of anthropogenic emissions on air pollution have been thoroughly investigated in past decades, yet the contribution from maritime shipping remains largely poorly documented. The study applied a solid modelling method with detailed discussions of the results and clear conclusions. In general the manuscript is well organized with good quality. Therefore, I would recommend the manuscript to be accepted with a minor revision, if the following comments could be properly addressed.

Author's Response:

We thank the anonymous reviewer for investing their time in a thorough review of our manuscript. Below, we provide a point-by-point response to all the concerns raised by this reviewer. Reviewer's comments appear in bold font and our responses are given in regular font. Changes to the manuscript are given in blue font.

Main comment#1.

1. **The manuscript lacks an evaluation section to demonstrate the performance of CAMx, which leaves the uncertainty remains unknown. It is necessary to show a discrepancy between simulation and observation so that the simulated contribution from shipping emissions can be properly interpreted.**

Author's Response:

We would like to thank the reviewer for their valuable suggestions. We believe that for differences between the two cases, the evaluation will not impact the results as much. That is because both scenarios are run with the same exact model setup and the only difference between the two sets of runs, is the presence and absence of the ships. For that reason, if a pollutant is under/overestimated in one set of runs with the ships, it is also under/overestimated in the other set of runs without the ships. However, due to the non-linear and complex nature of the atmosphere, and to maintain transparency in our research and with respect to the reviewer's comment, we have completed the analysis on model performance evaluation and have added it as a section (CAMx model performance analysis) to our paper as follows:

> *"***CAMx model performance analysis**
>
> The primary goal of this study is to explore changes to pollution levels between the two examined case studies, one involving the presence of ships and the other without. Despite the instances where CAMx may either under or overestimate pollutant concentrations, it is noteworthy that the model bias remains the same in both scenarios. Consequently, we hold

the view that these outcomes are unlikely to have a significant influence on our analysis. Nevertheless, we have thoroughly evaluated the model's performance to maintain transparency in our findings. It's important to acknowledge that uncertainties in air quality modeling can arise from various sources, such as uncertainties in emission inventories (Foley et al., 2015), the accuracy of meteorological inputs (Kumar et al., 2019; Ryu et al., 2018; Zhang et al., 2007), numerical noise inherent in the model (Ancell et al., 2018; Golbazi et al., 2022), and numerical approximations.

For our evaluation process of these four pollutants, we rely on measurement data sourced from the Environmental Protection Agency (EPA) AirNow program, which is publicly accessible (https://aqs.epa.gov/aqsweb/documents/data_api.html). Within the geographical scope of our study, we have access to data from a network of monitoring stations. Specifically, there are a total of 196 stations providing data for ozone (O3), and 87, 73, and 118 stations supplying data for SO2, NO2, and PM2.5, respectively. This extensive dataset forms the basis of our assessment, enabling us to comprehensively evaluate the CAMx model's performance in replicating real-world air quality conditions for these pollutants. It is worth mentioning that evaluating PM2.5 presents challenges due to the nature of EPA-reported PM2.5 measurements in the AirNow database. These values are directly obtained through instrumental measurements, classifying any particle smaller than 2.5 micrograms as a PM2.5 species. This method doesn't provide a clear means of distinguishing between the various particles detected by these instruments. In contrast, the PM2.5 species in our study are defined based on CAMx model documentation (Rambol Environment and Health, 2020). This divergence in approach makes a comprehensive PM2.5 evaluation challenging and pursuing alternative assessment methods falls beyond the scope of our current study.
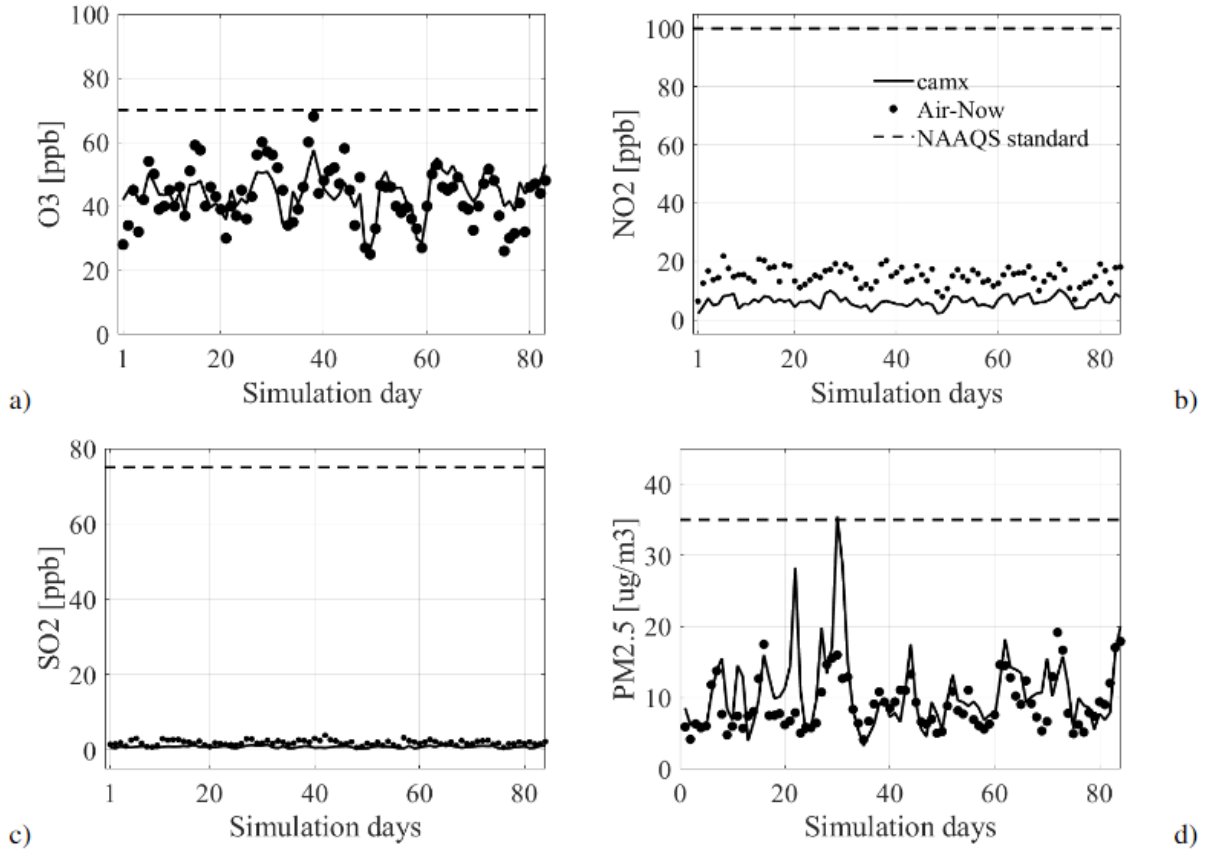
Figure 3., Model bias time series; CAMx model performance evaluated against the AirNow measurements; MBE is calculated across all stations at each day a) O3 [ppb], b) NO2 [ppb], and c) SO2 [ppb], and d) PM2.5 [µg/m3].

Figure 3 illustrates a time series of the AirNow measurements across the simulation days (in black circles), as well as the co-located CAMx outputs for the pollutant of interest in the solid black line. The co-located data are such that they are extracted at the same hour as observations and at the mass point of the grid cell that contains that specific station. Figure 4, on the other hand, illustrates the mean bias error (MBE) calculated at every station and depicts a spatial distribution of the model MBE for each pollutant using the co-located data.

CAMx demonstrates a tendency to slightly under- or over-estimate O3 concentrations closer to the coast, and away from the coast, respectively (Figure 2a). Our focus is mainly on locations closer to the coast since that is where we detect the highest impact of shipping emissions. For O3, a calculated MBE of -1.12 ppb indicates a systematic underestimation of around 2.5% across all monitoring stations within the designated domain. Overall, the model effectively captures the O3 trend and demonstrates a satisfactory level of agreement with observational data, as illustrated in Figure 1a. In addition, CAMx showcases a strong alignment with observational data in terms of SO2 simulations with minimal deviation from the observations.
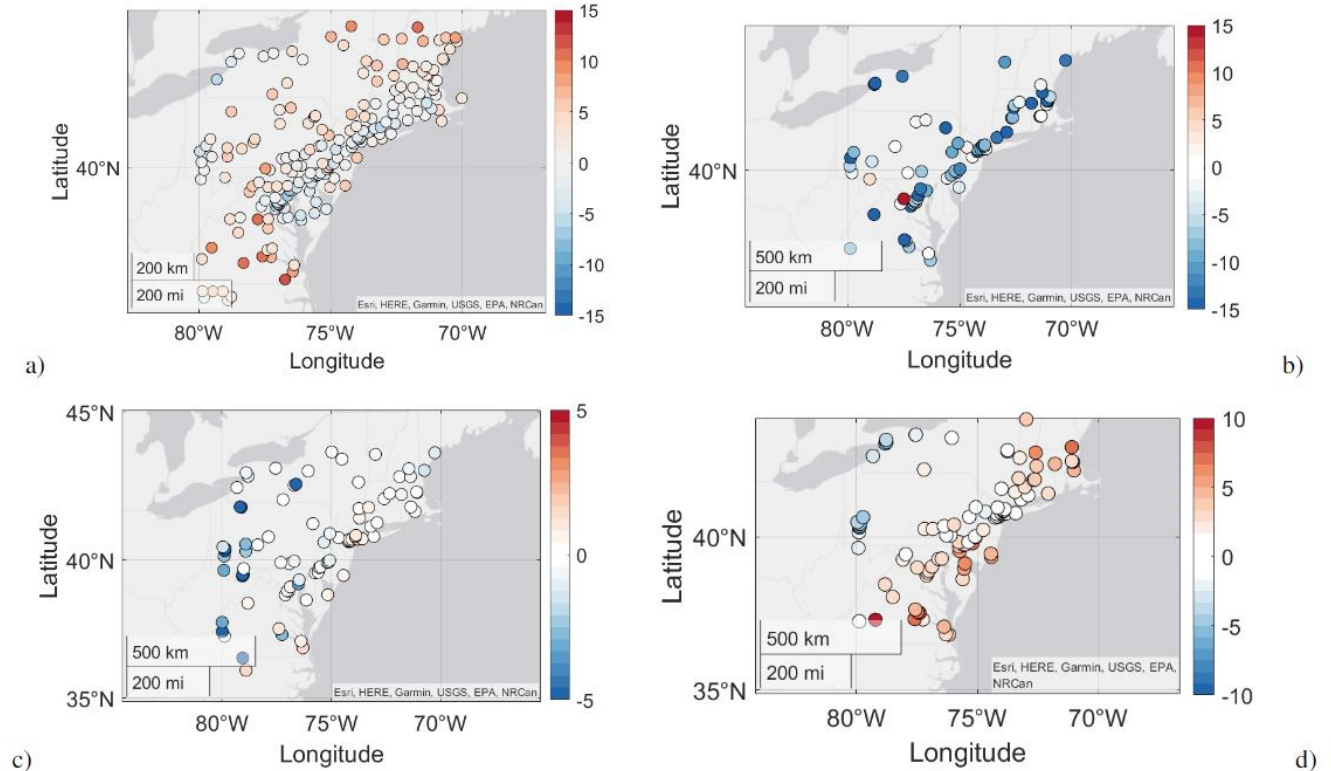
Figure 4. CAMx model performance against the AirNow observations; MBE calculated at each station for a) O3 [ppb], b) NO2 [ppb], and c) SO2 [ppb], and d) PM2.5 [µg/m3]. Blue shades show a systematic underestimation, while the red shades illustrate a systematic overestimation by the model.

For PM2.5, the model typically underestimates high PM2.5 episodes, as is commonly observed in prior studies (Delle, 2020; Golbazi, 2023). Nonetheless, for the remainder of the time, it demonstrates a strong alignment with observed data, as shown in Figure 3d. Figure 2d reveals that the model bias for PM2.5 consistently remains below 5 µg/m3 for the majority of coastal stations, with only a few exceptions.

Shifting focus to NO2, the model systematically underestimates NO2 concentrations (Figure 3b, and Figure 4b). This observation aligns with findings reported in existing literature (Ma et al., 2006). The notable underestimation of NO2 levels within the model can be attributed to the fact that the monitoring stations are typically situated in close proximity to major roadways characterized by heavy traffic flow, resulting in elevated NO2 emissions. Conversely, NO2 concentrations at locations farther away from these monitoring stations tend to be significantly lower than those recorded by the sensors near high-traffic roads (Figure 2a). On the other hand, in the CAMx model, data is extracted from the nearest central mass point within a grid cell containing the AirNow station's location, providing an averaged representation of NO2 levels within that specific grid cell. Consequently, the inherent positive bias in observations contributes to the model's tendency to underestimate this pollutant."

Main comment#2.

2. **Another issue with the manuscript is the lack of necessary discussion about the diurnal variational and seasonality of shipping emissions on coastal air quality. Wind patterns differ significantly between day- and night-time and this may play an important role in coastal cities air quality as it affects both chemistry and dispersion. For example, it may alter the NOx and VOC relative ratio, and bring excessive chlorine from the ocean to urban. Fig.5 showed a diurnal pattern of O3, but no in-depth discussion was given to explain the diurnal changes. For the same reason, the contribution from shipping emissions may be also different between summer and winter. Therefore, I would recommend the manuscript to include at least a brief discussion regarding this seasonality according to other studies, if adding a winter simulation was not feasible.**

Author's Response:

We agree with the reviewer that ships will have different impacts during different seasons. However, our main focus in this study is O3 pollution on the East Coast which is directly affected by temperature, solar radiation, wind speed, and other meteorological factors. For this reason, we base our study on summer when the highest O3 episodes occur. In addition, the emission inventory from the EPA was limited to April – October of 2018 and it was not possible to extend our study to create winter simulations. We understand that a seasonality analysis of the ship impacts would be a valuable addition, however, as the reviewer has noted, due to the computational costs of the simulations and limitations on the emissions, it is not feasible at this time to repeat our simulations for other seasons. To cover this topic, however, we explored this matter in the literature. To the best of our knowledge, there aren't many studies exploring shipping pollution in the United States. However, we found fundamental studies that are conducted for other regions in the world, or on a global scale and have added the paragraph below about their findings for the seasonal variations of the shipping impacts. To organize the order of the topics with the new addition to the "Introduction" section, we have re-ordered the last few paragraphs in the "Introduction" after adding the new studies. The new addition to our introduction reads as follows in the revised paper:

> "Seasonal variations in the impact of shipping on various pollutants have been documented in prior studies. For example, Eyring et al. (2010) noted that during Mediterranean summer conditions, characterized by slow atmospheric transport, strong solar radiation, and limited washout, primary ship emissions accumulate, and secondary pollutants form. They reported that secondary sulfate aerosols from shipping were responsible for 54% of the average sulfate aerosol concentration in the region during the summer. Our findings along the US East Coast align with their finding, highlighting the substantial contribution of ships to SO2 pollution during the summer season.
>
> Furthermore, they observed that in winter, shipping NOx emissions could lead to ozone depletion in northern Europe. In a separate study, Eyring et al., (2007) noted significant variations in simulated O3 levels between January and July, despite a consistent ship emission inventory throughout the year. They found that during winter, additional NOx emissions from shipping led to O3 reduction due to titration, while in summer, these emissions resulted in relatively modest but positive O3 concentration changes in regions with sufficient solar radiation. In addition, they show that the highest ship impacts on O3 due to the ship emissions were found in July and April, whereas in October and January, the

In response to the reviewer's feedback concerning the analysis of diurnal changes in the impact of shipping emissions on the pollutants, we generated a time series representing these impacts. Constructing a diurnal data series required employing statistical methods, including averaging data across the other two dimensions out of the three (averaging over days and locations).

However, it's crucial to note that averaging ship impact data across all grid cells would obscure the true impact, as ships primarily affect specific grid cells near the coast, and including unaffected grid cells would impact our statistics. To avoid this issue, we strategically selected four specific coastal locations, each corresponding to a significant city or major port. For each pollutant, we extracted the time series data from these chosen locations (as shown in Figure 11 in the new revision). This selection was made to ensure the representation of large urban areas and key ports in our analysis. Below, we provide additional context including our findings regarding the diurnal impacts.

"In order to examine the diurnal variations in the impact of shipping activities on each of the four pollutants, we generated time series data representing the daily cycles of changes induced by ships. To achieve this, we specifically chose four key locations along the eastern coast: Manhattan, New York; Baltimore, Maryland; Boston, Massachusetts; and Norfolk, Virginia. This selection was deliberate, as these locations encompass large cities as well as major ports, making them suitable representatives for assessing the shipping-related effects on air quality.

Figure 11. Diurnal cycle of the ship emission impacts on pollutants for a) SO2 [ppb], b) NO2 [ppb], c) O3 [ppb], d) PM2.5 [µg/m3]. The first through fourth columns represent changes in Manhattan, NY, Baltimore, MD, Boston, MA, and Norfolk, VA, respectively.

The dashed lines are the 25th and 75th percentiles, offering insights into the distribution of the impacts across various days and stations at each simulation hour. In contrast, the solid pink line represents the median impact attributed to the presence of ships.

For both NO_2 and SO_2, we observe an increase in concentrations when ships are present at all hours, as evidenced by the positive values of the median diurnal impact. Notably, the most significant impact for NO_2 is observed around 05:00 – 15:00 UTC (corresponding to 01:00 to 11:00 local time). For SO_2, we do not detect a clear diurnal pattern across all four locations. The median changes in O_3 levels show varying patterns across different locations. In Baltimore, MD, and Norfolk, VA, the median impacts on O_3 are minimal. In Manhattan, NY, O_3 levels demonstrate consistent negative changes across all hours, indicating a reduction in O_3 concentration in the presence of ships, with the most pronounced decrease occurring between 05:00 - 12:00 UTC (equivalent to 01:00 - 08:00 local time). It's important to note that these values represent the 8-hour average O_3 concentrations, meaning that, for instance, 08:00 local time represents the average O_3 levels between hours 08:00 and 16:00. Conversely, in Boston, MA, the most significant impacts of ships on O_3 levels are observed between 11:00 and 20:00 UTC (equivalent to 07:00 - 16:00 local time) and are increased. $PM2.5$ shows a similar diurnal pattern to NO_2 as it shows a positive impact (increase in $PM2.5$ levels by the ships) in all hours, with the highest impact during the ~ 00:00 – 12:00 UTC (corresponding to ~ 20:00 to 08:00 local time). Apart from Manhattan, NY, where the highest impacts occur around hour 20:00 UTC (16:00 local time).

It is worth highlighting that the influence of shipping emissions on the four pollutants shown in Figures 6–9 (b-c) may be different than the findings in Figure 11. This divergence arises from our utilization of distinct metrics in these two analyses. In Figure 11, we base our assessment on median impacts within the four locations, whereas in the other figures, we evaluate the impacts with regard to EPA regulations or under a worst-case scenario."

Main comment#3.

3. **Another main issue with the manuscript is lack of thorough discussion of biomass burning impact on precipitation. First, biomass burning intensity was not clearly described. Fig.7 showed fire spot on Nov.25, but the study period is Dec.14-19, the gap is too long to indicate the rapid changes of both fire and precipitation. There is no demonstration about fire emission 2~3 days prior to the study period, assuming the extreme precipitation may turn off the local biomass burning. Second, to distinguish the impact of biomass burning aerosol, it is necessary to explain the influence of using diagnostic aerosol first. This would help to understand the relative contribution from anthropogenic aerosol and biomass burning emissions.**

Author's Response:

It seems like this comment is not relevant to our study. The comment is for Figure 7 which shows a fire spot for Nov 25. The reviewer mentions that our analysis is for Dec 14-17.

Our study spans over 3 months of summer in 2018, and we do not present any results for Nov 25. In addition, Figure 7 in our study shows the "a) percentage of the times when $\Delta H2O2/\Delta HNO3 < 0.35$ as determined in the CAMx model, which is an indication of a VOC-limited regime; b) maximum contribution of ships to O3 pollution (Figure 6c); and c) same as in b) but for NO".

Minor comment#1.

4. **It's necessary to describe the vertical layer configuration (e.g., first layer height) to demonstrate that the near-surface layers can properly resolve the stack heights of shipping emissions.**

Author's Response:

We appreciate the reviewer's concern on this important matter. We have corrected the statement below to include our model configuration in vertical as well as in horizontal directions:

"The meteorological files have 400 x 400 horizontal grid points covering the entire CAMx domain, which consists of 315 x 300 grid points, the same as the emission files. We impose 35 vertical levels that are closely spaced near the surface and then gradually expand. The top hydrostatic pressure is 20 hPa and the lowest model level is at approximately 3.5 m above mean sea level (AMSL). Details about the model configuration are discussed in Table 1."

We have also added the height of the lowest model level to Table 1 in the revised paper.

NOTE: We updated the conclusions as needed for the updates as follows:

"Ships emit significant amounts of pollutants within 400 km of the shores. Here, we studied the ocean-going ship emissions on the air quality of the U.S. East Coast. We utilized the WRF-CAMx modeling system to simulate the pollution concentrations in the presence and absence of shipping activities along the East Coast and at the major ports. We used the WRF model to provide the meteorological inputs for the CAMx air quality model for the year 2018, on which the most recent EPA/NEI emission inventory is based. We particularly focused on PM2.5, SO2, NO2, and O3.

Overall, we studied the outcomes of every pollutant from two perspectives: 1) from the EPA perspective concerning the national concentration standards for each specific pollutant, and 2) the maximum contribution of ships to that pollutant over the 3 months. Our assessment of the CAMx model's performance reveals strong performance in simulating SO2 levels. The model shows a slight underestimation of O3 concentrations near the coast and a slight overestimation farther from the shore. Nevertheless, the mean bias error for O3 is limited to -1.12 ppb. Likewise, the bias in PM2.5 concentrations remains below 5 µg/m3. On the other hand, the model exhibits a noticeable underestimation of NO2 concentrations, primarily stemming from a positive bias in observations collected in proximity to major roads.

We find that shipping increases the PM2.5 concentrations across the domain. the 98-th percentile daily average PM2.5 levels increased by 3.2 µg/m3 over the ocean and in some coastal areas. However, in a worst-case scenario, ships contribute up to approximately 8.0 µg/m3 to PM2.5 concentrations, only over the Atlantic off the coast of MD, and VA. In addition, we find that ships have a significantly high impact, up to 95% and 90%, on the SO2 concentrations over the Atlantic and inland, respectively. This suggests that the CMV sector is one of the highest contributors to SO2 levels in the region. The shipping contribution to SO2 levels was up to 45 ppb over coastal regions. Ship emissions also impacted the NO2 design value by up to 34 ppb. In addition, our simulation results show that the impact of ship emissions on O3 concentrations is not uniform, meaning that maritime shipping affects ozone pollution in both positive and negative ways. Although over the ocean O3 concentrations increase significantly in the presence of ships (up to 8.6 ppb), in coastal areas with major cities and major ports O3 concentrations decrease by up to ~6.5 ppb. To understand the reasons behind the O3 reduction in the presence of ships, we analyzed the $\Delta H2O2/\Delta HNO3$ ratio in the region, which is used to determine NOx- or VOC-limited ozone production, as well as changes to NO concentrations, since they play a significant role in O3 formation and destruction. We found that ships emit significant amounts of fresh NO in the atmosphere, which then helps scavenge O3 in VOC-limited regimes. As a result, with higher NO concentrations in the atmosphere produced by ship emissions, O3 is destructed in major cities and urban areas. By contrast, over the ocean (a NOx-limited regime), excessive NOx emissions due to the ships contribute to the formation of O3 and therefore an enhancement in O3 concentrations. It is important to note that the destruction of O3 by ship emissions in major cities does not necessarily mean that the ships create better air quality because a decrease in O3 is a consequence of a significant increase in other pollutants, like NO. The diurnal cycle in the impact of shipping emissions across four major cities shows different patterns for different locations. For instance, the highest impacts on O3, occur at different times for different locations. PM2.5 and NO2, however, experience the highest changes in early morning in most locations. On the other hand, we do not detect consistent patterns for changes in SO2.

Overall, the majority of the time, due to the dominant southwesterly wind direction in the region, the impacts on different pollutants remained spatially confined offshore. However, in some coastal areas near the major ports, the impacts were significant."

We corrected the references by adding the new studies (below) used in our paper:

1. Ancell, B. C., Bogusz, A., Lauridsen, M. J., and Nauert, C. J.: Seeding Chaos: The Dire Consequences of Numerical Noise in NWP Perturbation Experiments, Bulletin of the American Meteorological Society, 99, 615 – 628, https://doi.org/10.1175/BAMS-D-17-0129.1 ,2018.
2. Delle Monache, L., Alessandrini, S., Djalalova, I., Wilczak, J., Knievel, J. C., and Kumar, R.: Improving air quality predictions over the United States with an analog ensemble, Weather and Forecasting, 35, 2145–2162, 2020.

3. Eyring, V., Isaksen, I. S., Berntsen, T., Collins, W. J., Corbett, J. J., Endresen, O., Grainger, R. G., Moldanova, J., Schlager, H., and Stevenson, D. S.: Transport impacts on atmosphere and climate: Shipping, Atmospheric Environment, 44, 4735–4771, 2010a.

4. Eyring, V., Stevenson, D. S., Lauer, A., Dentener, F. J., Butler, T., Collins, W. J., Ellingsen, K., Gauss, M., Hauglustaine, D. A., Isaksen, I. S., et al.: Multi-model simulations of the impact of international shipping on Atmospheric Chemistry and Climate in 2000 and 2030, Atmospheric Chemistry and Physics, 7, 757–780, 2007b.

5. Foley, K. M., Hogrefe, C., Pouliot, G., Possiel, N., Roselle, S. J., Simon, H., and Timin, B.: Dynamic evaluation of CMAQ part I: Separating the effects of changing emissions and changing meteorology on ozone levels between 2002 and 2005 in the eastern US, Atmospheric Environment, 103, 247–255, 2015.

6. Golbazi, M., Kumar, R., and Alessandrini, S.: Enhancing air quality forecasts across the contiguous United States (CONUS) during wildfires using Analog-based post-processing methods, Tech. rep., Copernicus Meetings, 2023.

7. Kumar, R., Lee, J. A., Delle Monache, L., and Alessandrini, S.: Effect of meteorological variability on fine particulate matter simulations over the contiguous United States, Journal of Geophysical Research: Atmospheres, 124, 5669–5694, 2019.

8. Liu, H., Fu, M., Jin, X., Shang, Y., Shindell, D., Faluvegi, G., Shindell, C., and He, K.: Health and climate impacts of ocean-going vessels in East Asia, Nature climate change, 6, 1037–1041, 2016.

9. Ma, J., Richter, A., Burrows, J. P., Nüß, H., and van Aardenne, J. A.: Comparison of model-simulated tropospheric NO2 over China with GOME-satellite data, Atmospheric Environment, 40, 593–604, 2006.

10. Ramboll Environment and Health: COMPREHENSIVE AIR QUALITY MODEL WITH EXTENSIONS Version 7.10 – User's guide, Tech.rep., https://camx-wp.azurewebsites.net/Files/CAMxUsersGuide_v7.10.pdf, 2020 .

11. Yao, Z., Wu, B., Shen, X., Cao, X., Jiang, X., Ye, Y., and He, K.: On-road emission characteristics of VOCs from rural vehicles and their ozone formation potential in Beijing, China., Atmospheric Environment, 2015.

12. Zhang, F., Bei, N., Nielsen-Gammon, J. W., Li, G., Zhang, R., Stuart, A., and Aksoy, A.: Impacts of meteorological uncertainties on ozone pollution predictability estimated through meteorological and photochemical ensemble forecasts, Journal of Geophysical Research: Atmospheres, 112, 2007.

This manuscript offers an assessment of the effects of shipping emissions on air quality along the eastern coast of the United States pointing to substantial impacts within certain regions. I found the discussion to be well-reasoned and insightful, especially when tackling the dynamics between nitrogen oxides, ozone, and VOCs. Also, the perspective added by the authors on meeting the emission regulations currently in place in the U.S. is quite relevant. Thus, with a minor revision addressing the subsequent remarks, I am inclined to recommend its acceptance.

Author's Response:

We thank the anonymous reviewer for investing their time in a thorough review of our manuscript. Below, we provide a point-by-point response to all the concerns raised by this reviewer. Reviewer's comments appear in bold font and our responses are given in regular font. Changes to the manuscript are given in blue font.

1. **These include a more detailed introduction of the emission inventories (e.g., what anthropogenic sources have been included? And what quantity?), so the reader can better understand the share of shipping within the region studied.**

Author's Response:

About the emission inventory, we originally included a subsection (Emission Data) under the Methods section. However, we realized that it is short and may not be clear. In the original submission, we had:

> "*In the 2018 NEI data, the gridded 2D emissions are merged, meaning that they are provided as one set of surface emissions that include all emission sectors. On the other hand, the elevated point sources are provided for each potential sector separately. For ship emissions, we use the emission data for the Commercial Marine Vessels (CMV) sector, which includes Category 1, 2 (small engine), and 3 (large engine) ships. CAMx computes the time-varying buoyant plume rise using stack parameters and the hourly emissions for each emissions sector, including CMV. Unlike previous EPA data sets, the CMV emissions in 2018 are at a one-hour temporal resolution. The initial and boundary conditions for this study are also provided by the EPA.*"

To address the reviewer's concern, we have now expanded this paragraph about the emission inventory and different sectors within it as follows:

> "The 2018 NEI data is based on the year 2017 activity. It contains merged gridded 2D surface emissions, meaning that they are provided as one set of surface emissions that include all the existing 2D emission sectors, i.e., anthropogenic emissions including aircraft emissions, on-road and non-road emissions, railroad emissions, and agricultural emissions. It also includes biogenic emissions. The 2018 inventory lacks the wildfire emissions for this time and domain. However, Our investigation through the wildfire history showed that 2018 was a year with a

low number of wildfires especially along the East Coast (https://www.nifc.gov/fire-information/statistics/wildfires) and therefore we do not believe this to significantly impact our findings. Nonetheless, in future studies, including wildfire emissions upon availability is recommended. In contrast to the 2D grided emissions, the elevated point sources in this inventory are provided for each sector, separately.

For the ship emissions, we use the emission data for the Commercial Marine Vessels (CMV) sector, which includes Category 1, 2 (small engine), and 3 (large engine) ships. These emissions are calculated based on the ship's fuel consumption, ship engine type, ship activity, and emission factors specific to those characteristics. EPA's CMV estimates are computed using detailed satellite-based automatic identification system (AIS) activity data from the US Coast Guard (EPA, 2021, 2020). Other point sources present in this inventory include electric generation units, point oil, and gas sources, and any other point sources. CAMx computes the time-varying buoyant plume rise using stack parameters and the hourly emissions for each emissions sector, including CMV. Unlike previous EPA data sets, the CMV emissions in 2018 are at a one-hour temporal resolution, which is very important and makes this study the first to utilize hourly emissions for the ships. The initial and boundary conditions for this study are also provided by the EPA and are products of the GEOS-Chem model."

2. **A map with the spatial representation of those emission inventories would also be relevant to understanding how the concentrations change compared to where emissions occur.**

Author's Response:

The reviewer brings up a valuable point that showing a map distribution of emissions would help understand the changes in concentrations compared to the emissions. However, an illustration of the spatial distribution of all emissions is challenging, in that, the emissions are provided in different formats (2D emissions and elevated point sources). In addition, in the 2D gridded emissions, several pollutants are included which are primary pollutants. With respect to the reviewer's comment, we produced maps of the 2D gridded emissions. But out of the four pollutants that we study here, only two (NO2 and SO2) are directly emitted into the atmosphere and therefore are included in emission data. We provided the plots for those two pollutants and added them to the "Emission Data" section with the description below:
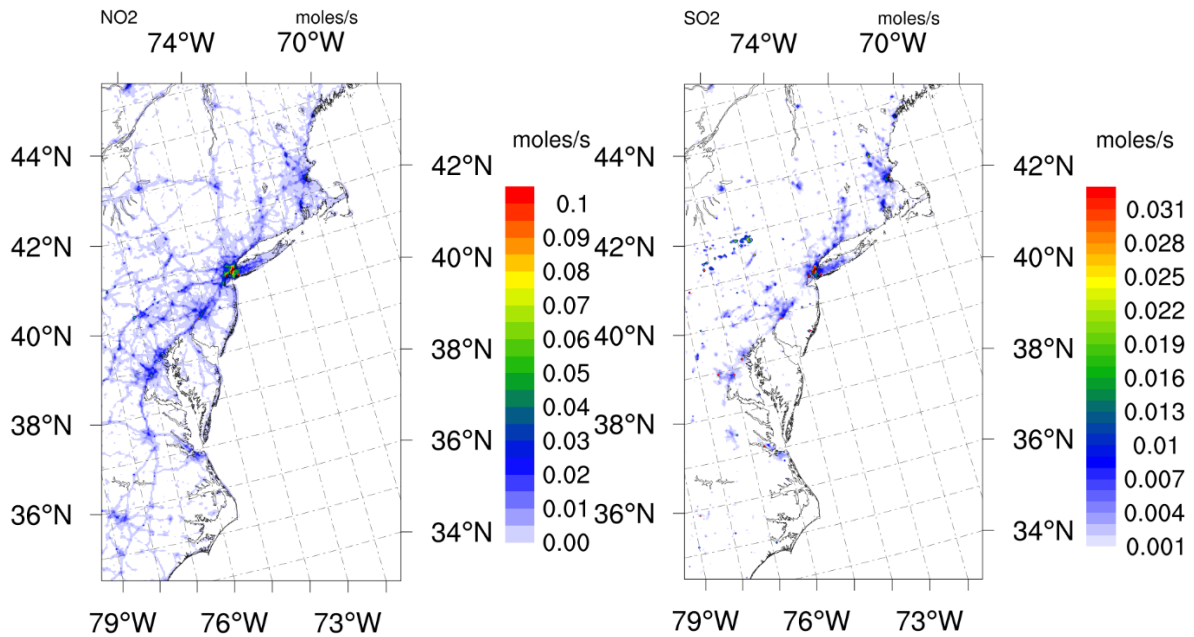
Figure 2. Gridded 2D emission distribution across the domain (averaged over three months) in moles/s for a) NO2, and b) SO2. The gridded emissions include all the 2D anthropogenic and biogenic emissions and exclude the elevated point sources.

"The spatial distribution of the 2D gridded merged anthropogenic emissions are illustrated in Figure 2. It's important to note that O3 is a secondary pollutant, meaning it isn't directly emitted into the atmosphere. Conversely, PM2.5 is either a primary or secondary pollutant. Hence, we have specifically generated gridded emission maps for NO2 and SO2, only. The distribution of NO2 emissions closely mirrors the pattern of major highways and roads, as transportation stands out as one of the most significant sources of nitrogen oxide (NOx) emissions. The objective of this figure is to explain the spatial distribution of gridded anthropogenic emissions, shedding light on how concentrations change (Figures 6a and 7a) in relation to their emission sources."

3. **In addition, if authors are willing to discuss the impact of shipping in different U.S. states, it would be relevant to include their location and name in at least one figure to contextualize the non-American readership.**

Author Response:

Thanks for bringing this point up, we have added names of some important locations to the map of the domain for unfamiliar readers.
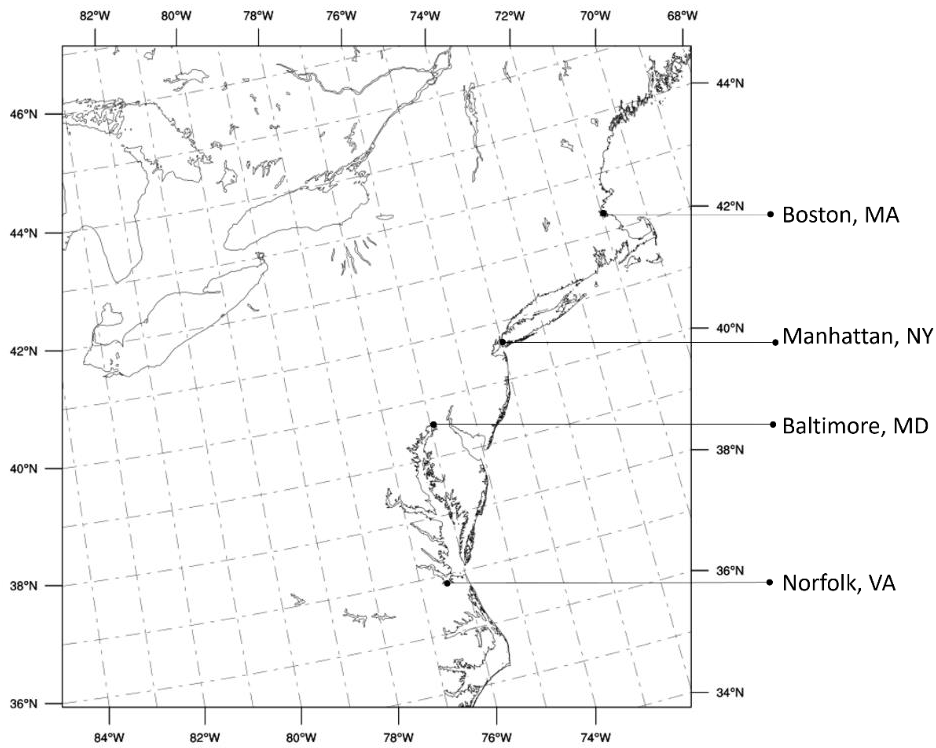
We added the references below to the paper:

1. U.S. Environmental Protection Agency: 2020 National Emissions Inventory Technical Support Document: Commercial Marine Vessels, Tech.rep., https://www.epa.gov/system/files/documents/2023-03/NEI2020_TSD_Section11_CMV.pdf, 2020.

2. U.S. Environmental Protection Agency: 2017 National Emissions Inventory: January 2021 Updated Release, Technical Support Document, Tech. rep., https://www.epa.gov/air-emissions-inventories/2017-national-emissions-inventory-january-2021-updated-release-technical, 2021.